University of Washington
Department of Civil and Environmental Engineering

LINEAR AND NON-LINEAR DYNAMIC RESPONSE OF FLOATING BREAKWATERS IN DIRECTIONAL SEAS

Senaka C.B. Ratnayake
Derald R. Christensen
Ronald E. Nece
Billy J. Hartz

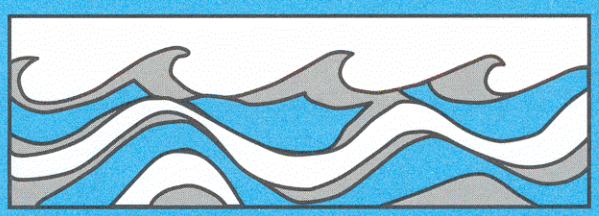

Water Resources Series
Technical Report No. 90
October, 1984

Seattle, Washington
98195

Department of Civil Engineering
University of Washington
Seattle, Washington 98195

LINEAR AND NON-LINEAR DYNAMIC RESPONSE OF FLOATING BREAKWATERS IN DIRECTIONAL SEAS

Senaka C.B. Ratnayake
Derald R. Christensen
Ronald E. Nece
Billy J. Hartz

Water Resources Series
Technical Report No. 90

October 1984

University of Washington
Department of Civil Engineering
Environmental Engineering and Science Program
Seattle, Washington 98195

LINEAR AND NON-LINEAR DYNAMIC RESPONSE OF FLOATING BREAKWATERS IN DIRECTIONAL SEAS

by

Senaka C.B. Ratnayake
Derald R. Christensen
Ronald E. Nece
Billy J. Hartz

Water Resources Series
Technical Report No.90
October 1984

Project Title: Floating Breakwater Prototype Test Monitoring Program, West Point, WA

Contract No. : DACW67-81-C-0196

Principal Investigators : Derald Christensen
Senior Research Associate
Ronald E. Nece
Professor
Eugene P. Richey
Professor
Department of Civil Engineering
University of Washington

TABLE OF CONTENTS

NOTATION

A	- Submerged section area of structure
$\mathbf{A}$	- Hydrodynamic mass of the structure
$\mathbf{A}^e$	- Hydrodynamic mass of the finite element
$\mathbf{a}$	- (Two dimensional) hydrodynamic mass of the cross section
B	- Width of structure section
$\mathbf{C}$	- Hydrodynamic damping matrix of the structure
$\mathbf{C}^e$	- Hydrodynamic damping matrix of the finite element
$\mathbf{c}$	- (Two dimensional) hydrodynamic damping of the cross section
$E[x]$	- Expectence (or, ensemble average) of x
$\mathbf{F}$	- Force vector
f	- frequency in hertz.
$\mathbf{f}$	- Hydrodynamic exciting force transfer matrix.
$\mathbf{K}$	- Structure stiffness matrix
$\mathbf{K}'$	- Hydrodynamic buoyancy stiffness matrix
$\mathbf{K}'^e$	- Hydrodynamic buoyancy stiffness of finite element
k	- Wave number
$\mathbf{k}$	- Wave number vector = $k[\cos\theta, \sin\theta]$
$\mathbf{k}'$	- (Two dimensional) hydrodynamic buoyancystiffness of the cross section
L	- Total length of the structure
l	- Length measured along an element
l_e	- Finite element length

M - Mass matrix of the structure

m - Cross sectional mass matrix (two dimensional)

N - Interpolation matrix (in finite elem. analysis)

n - Unit normal to the structure surface

p - Pressure

Q - Cross power spectral density matrix

Quadratic moment transfer function vector

R - Matrixof body to global coordinatetransformation

Response transfer function matrix for the structure

r - Complex phase lag vector for directional wave gages

- Structure response vector

S - Structure section boundary

$S_{\eta}(w)$ - Uni-directional wave spectrum

$S_{\eta}(\theta,w)$ - Directional wave spectrum

$\mathbf{S}_{F2}$ - Drift force spectral matrix

$\mathbf{S}_{r2}$ - Drift response spectral matrix

s - First order displacement of the center of gravity of the cross section

t - time

T - Draft

T - Quadratic drift force transferfunction vector

U - Quadratic transfer function vector for sway force and roll, yaw moments only.

w	- Wave frequency
$\mathbf{x}$	- Cartesian coordinate vector (x,y,z)
$\mathbf{x}_i$	- Position vector of directional wave gage i
η	- Incident wave height
Φ	- Velocity potential
ϕ	- Space dependent velocity potential, roll disp.
	- Inclination of anchor cable to the horizontal.
ρ	- Density of water
Γ	- Fluid flow field boundary
θ	- Angle of wave approach measured from the normal to the structure
ε	- Random phase angle
μ	- Difference wave frequency for a pair of wave fronts
ψ	- Difference angle for a pair of wave fronts
ζ	- Spatial lag vector
τ	- Time lag

Subscripts

n,m	- Any quantity related to wave fronts n and m respectively

Superscripts

e	- Element quantity
T	- Transpose of a vector or matrix
*	- Conjugate of a complex quantity

LIST OF TABLES

LIST OF FIGURES

CHAPTER 1

Introduction and Background

1.1 Introduction

During the past years the interest and research on the design and performance of floating breakwaters has been growing steadily. Conventional breakwaters, such as seawall and rubble-mound types are best suited for shallow water. A floating breakwater with an anchor system is more practical and less expensive for deep water sites or where sea foundation is poor. Floating breakwaters also have environmental advantages because their construction does not severely affect water circulation and hamper marine life and fish migrations or littoral transport.

The ability to predict the motion response (and consequently the forces and moments) to a given wave field is animportant first step in the design of floating structures. It is also an inexpensive alternative to more costly and time consuming physical model studies.

1.2 Previous Work

Various combinations of mathematical models and computer programs have been used in the past for floating structure analysis and the usage of ship motion programs was common. Two specific disadvantages were seen in this approach :

1) Long breakwaters could not be modelled, as the rigid body approach fails to give satisfactory results in this case.
2) Incorporation of the effects of mooring was difficult.

Adee, Richey and Christensen [1] came up with a two dimensional rigid body motion model with an extensive mooring analysis to obtain mooring spring constants. This gave conservative response estimates by assuming beam seas. They also carried out a partial treatment of non linear second order forces on the structure. Hartz and Georgiadis [20]developed an efficient model for analysis of flexible floating structures. Good predictions were made by this model assuming that the wave coherence along the breakwater is modelled well enough and neglecting the coupling between sway and roll motions. Hutchison [27] used the output produced by the NSRDC (Naval Ship Reasearch Development Center) ship motion program as the input to a post-processing program to predict the motion of moored floating breakwaters and barges. The analysis was again rigid motion type. Langen [34] developed a computer model to predict floating bridge behavior and considered directionally independent wave forces in the analysis. This could result in the overprediction of motions and forces.

An important factor that needs to be given more consideration is the effect of non-linear drift forces. Though this may not be a predominant factor in the design of the structure it self, it may be the single most important factor in the design of the mooring system.

Finally, all theoretical prediction models depend heavily on correct modelling of the sea state. It is now known that the wave directionality must to be taken in to account for such a sea

state model. The usual practice has been to assume that the directional wave spectrum can be written as

$$S_\eta(\theta,w) = S_\eta(w)\ \Psi(\theta) \qquad (1)$$

where $S_\eta(w)$ is the unidirectional wave spectrum, θ is the direction angle measured from any convenient datum. $\Psi(\theta)$ is the directional spread function having the property $\int_\theta \Psi(\theta)\, d\theta = 1$.

$\Psi(\theta)$ was approximated by $C*Cos^n(\theta - \bar{\theta})$, where C is a constant and $\bar{\theta}$ = mean wave direction. n was assumed to lie between 2 and 8 in most cases depending on the site. As described at a later stage of this report, field wave data indicates that this may not be the case in all instances. Note that as n becomes larger the directional spread function becomes narrower and the sea state approaches uni-directional condition.

1.3 The Research Project

Two years ago the Army Corps of Engineers contracted the University of Washington to a prototype floating breakwater monitoring program aimed at studying more about wave transmission characteristics, wave forces on the structure, anchor cable behavior, structure response and rubber connector behavior. In addition, boat-wake experiments were also carried out for various structure configurations. This gave the much desired opportunity to calibrate and compare a theoretical model with actual field data.

1.4 The Test Site

The test site for the floating breakwater monitoring program was located off West Point in Puget Sound (Fig. 1). Due to its exposed location, the wave and wind conditions were considered extremely suitable for such a project. The wind blew mostly from the north or south, which also meant that the wind direction was almost perpendicular to the breakwater (Fig. 2). This assured that the breakwater faced the worst conditions for any given sea state. The water depth at the site was approximately 50 ft. The fetch was about 9.0 and 6.8 miles from the north and south respectively.

1.5 Scope of the Problem

A numerical finite element model has been developed to analyze the behavior of long floating structures in a directional sea. It predicts coupled sway/roll and heave motions at a given number of nodes (or cross sections) using the sea state and structure configuration as inputs. In addition internal structure forces (shear and moments) can also be obtained at each node if required. The above model uses linear spectral techniques in the analysis and all the information are presented in spectral form so that the the designer can obtain important statistical information about the structure motion and relevant parameters. Model predictions have been compared with West Point field data and agreement was found to be close.

The second stage of the model, which is still under

development, will be used to predict the low frequency motion of comparatively short structures due to second order hydrodynamic forces (drift forces). This is an essential step in the design of mooring systems for short structures. The amount of data that has to be handled at this stage is enormous and so is the time required. The output of the first stage is used as the input to this model. A quasi-linear sepctral type analysis using quadratic transfer functions is used in the analysis (See Chapter 5).

CHAPTER 2

Data Acquisition and Analysis

2.1 Data Acquisition

A RCA microboard data acquisition system capable of sampling 96 data channels at a rate of up to 8 hz was developed for the study. A preliminary analysis of West Point data indicated that all the information at the site fell well below 2 hz (mosly below 1 hz). According to the theory of time series analysis, the sampling rate should be higher than or equal to twice the maximum frequency of the sampled data. A sampling rate of 4 hz was therefore considered sufficient. A linear wave gage array consisting of 8 probes, each 5 ft. apart (though in most cases only three were sufficient) to obtain directional wave data was installed well away from the structure to avoid reflection and diffraction effects (Fig. 3). Among other major measurements were, accelerations, wave pressure along the structure, relative motion between the pontoons, anchor loads, wind speed and wind direction.

2.2 Data Analysis

(a) Coordinate System

Fig. 3 shows the coordinate system and the wave probe locations used in the computation directional wave spectrum at the West Point site. The shown coordinate system was chosen only for convenience, but in general the origin can be any where on

the free surface and any general axis can be chosen as the reference direction.

(b) Directional Wave Spectrum

Introduction of high resolution Frequency - Wavenumber Spectrum analysis by Capon [8] for the analysis of seismic data and later utilized by others (e.g. Regier and Davis [50] and Oakley and Lozow [44]) for the analysis of water waves, greatly enhanced the capability of accurately describing the three dimensional sea. Maximum Likelihood Method (MLM), as it is widely called, was used in the analysis of West Point wave data. Capon [9], showed that MLM has much higher resolution than the more commonly used FFT method due to its higher noise rejection capability.

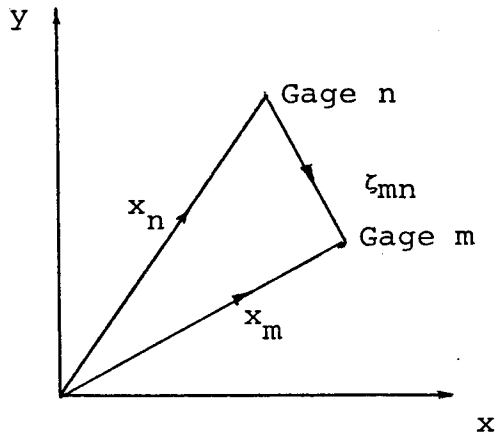

Refer to the above figure. Assuming that the wave height is a stationary stochastic process, it can be defined by the

stochastic integral [5], [15]

$$\eta(x,y,t) = \int_{-\infty}^{\infty} \exp[i(\mathbf{k}.\mathbf{x} - wt)]\, dZ_{\eta}(w,\theta)$$

where, $\mathbf{k} = (k\cos\theta, k\sin\theta)$ $\mathbf{x} = (x,y)$

$Z_{\eta}(\theta,w)$ is called the spectral process associated with the wave field with the following properties:

i) Orthogonal increments. i.e. $E[dZ_{\eta}(w,\theta)dZ^{*}_{\eta}(\mu,\Psi)] = \emptyset$ unless $w = \mu$ and $\theta = \Psi$.

ii) When $w = \mu$ and $\theta = \Psi$, $E[dZ_{\eta}(w,\theta)dZ^{*}_{\eta}(w,\theta)] = S_{\eta}(w,\theta)\, dwd\theta$

The space-time lag correlation by definition is given by,

$$C(\zeta,\tau) = E[\eta(\mathbf{x},t)\ \eta^{*}(\mathbf{x}+\zeta,\ t+\tau)]$$

Substituting the expression for (x,y,t) and using the relations in (i) and (ii) above,

$$C(\zeta,\tau) = \int_{\omega}\int_{\theta} S_{\eta}(\theta,w)\ \exp[i(w\tau - \mathbf{k}.\zeta)]\, d\theta\, dw$$

The spatially lagged frequency cross-spectrum Q is defined as,

$$Q(\zeta,w) = \int_{-\infty}^{\infty} C(\zeta,\tau)\ \exp(-iw\tau)\, d\tau$$

Substituting for C,

$$Q(\zeta,w) = \int_{\theta} S_{\eta}(\theta,w)\ \exp(-i\mathbf{k}.\zeta)\, d\theta$$

If there are N probes then the discrete expresssion for Q gives the Cross Power Spectral Density Matrix(CPSD) $Q_{mn}(\zeta_{mn},w)$.

$\zeta_{mn} = \mathbf{x}_n - \mathbf{x}_m$ and $\mathbf{x}_i$, $i = 1,2,..m,n,..N$ areprobe locations.

In other words, the element of CPSD in the m th row and n th column is equal to the cross spectrum between wave records at locations $\mathbf{x}_m$ and $\mathbf{x}_n$ respectively (see APPENDIX D). Other elements of the matrix correspond to the remaining ζ_{nm} values (or $\mathbf{x}_m$, $\mathbf{x}_n$ pairs). This can be directly constructed from wave

records of field data at the probes considered.

Now, if we consider a finite number (= M) of directions, the CPSD matrix can be written as,

$$\mathbf{Q} = \sum_{i=1}^{M} \mathbf{r}(w,\theta_i)\ \mathbf{r}^{*T}(w,\theta_i)\ S_\eta(w,\theta_i) \qquad (A)$$

where, $\mathbf{r}(w,\theta)$ is the complex phase lag vector that gives the phase lag between the origin and the probes ,

$$\mathbf{r}(w,\theta) = [\exp(i\mathbf{k}.\mathbf{x}_1) \quad \exp(i\mathbf{k}.\mathbf{x}_2) \quad \ldots\ ]$$

What we require is an inverse relation of (A) which gives an estimate $S_\eta(\theta,w)$ given $\mathbf{Q}$. Therefore we write [29]

$$S_\eta(\theta_d,w) = \mathbf{A}_d^{*T}\ \mathbf{Q}(w)\ \mathbf{A}_d \qquad (B)$$

Substituting for $\mathbf{Q}$ from (A) in (B),

$$S_\eta(\theta_d,w) = \sum_{i=1}^{M} \left|\mathbf{A}_d^{*}\ \mathbf{r}(w,\theta_i)\right|^2 S_\eta(\theta_i,w)$$

Coefficients of the vector $\mathbf{A_d}$ which minimize the right hand side contribution for i not equal to d gives the MLM estimate of $S_\eta(\theta_d,w)$. Or, we have to find $\mathbf{A_d}$ so that

$$S_\eta(\theta_d,w) = \left|\mathbf{A}_d^{*T}\mathbf{r}(w,\theta_d)\right|^2 S_\eta(\theta_d,w) + \sum_{i\neq d} \left|\mathbf{A}_i^{*T}\mathbf{r}(w,\theta_i)\right|^2 S_\eta(\theta_i,w)$$

is minimized subject to the constraint $\left|\mathbf{A}_d^{*T}\ \mathbf{r}(w,\theta_d)\right| = 1$. The resulting coefficients (see Appendix A for proof) form the MLM estimate of $S_\eta(\theta_d,w)$

$$S_\eta(\theta_d,w) = 1 \ /\ [\mathbf{r}^{*T}(w,\theta_d)\ \mathbf{Q}^{-1}(w)\ \mathbf{r}(w,\theta_d)]$$

In the case of a linear array, which is capable of resolving the directions only in the half plane of Ø - 18Ø deg or 18Ø - 36Ø deg, the wind direction gage was helpful in identifying the correct half plane, though this was actually not essential in the analysis of the structure. The advantage of using a linear array was the increase in directional resolution [45] , specially when the waves are approaching nearly normal to the array, which was found to be the case at the monitoring site. Figs.4 and 5 shows the directional sea state that existed on 1Ø/21/83 at ØØ:4Ø hrs. Fig. 6 and 7 shows the results of an attempt to fit a cosine spread function as described in Chapter 1. High values of n were obtained at some frequencies contrary to the usually expected low values. Miller [39] also confirmed that predicted structural response agreed with the measured response only for high values. This also meant that the assumption of beam seas would not introduce appreciable errors in this case.

CHAPTER 3

Hydrodynamic Loading on the Structure

A major and relatively time consuming part in the analysis process is the computation of the hydrodynamic loading, i.e. the computation of hydrodynamic mass, damping and direction dependent force coefficients. Assuming that the structure is "large" (relative to the wave length) the most suitable method appears to be the potential flow solution.

3.1 Coordinate and Boundary Definitions

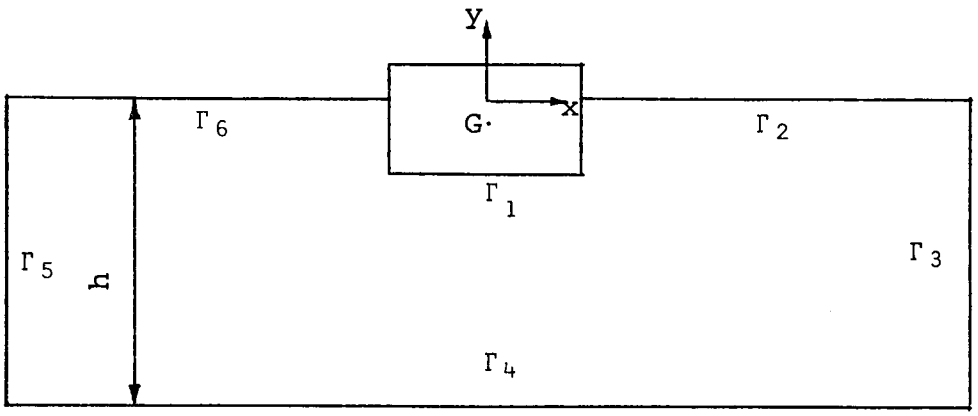

3.2 Equation Formulation

(a) Oscillation of the Structure at the Free Surface

The complex velocity potential produced by a harmonically oscillating floating structure can be described by

$$\Phi_j = \phi_j(x,y)\ \exp(-iwt)$$

where, j = 1,2,3 represents the small amplitude oscillation of

the structure in sway, heave and roll respectively given by

$$X_j = X_{j\emptyset} \exp(-iwt) \qquad i = 1,2,3$$

Φ_j should satisfy the following;

$$\nabla^2 \Phi_j = \emptyset \qquad \text{Laplace equation}$$

$$\partial^2 \Phi_j / \partial t^2 + g\, \partial \Phi_j / \partial y = \emptyset \qquad \text{at } y = \emptyset \text{ (free surface)}$$

$$\nabla \Phi_j = v_n \qquad \text{on the structure surface}$$

$$\partial \Phi_j / \partial y = \emptyset \qquad \text{at } y = -h \text{ (bottom)}$$

$$x \{\partial \Phi_j / \partial x + ik\Phi_j\} = \emptyset \qquad \text{when } x \to \infty \text{ (radiation condition)}$$

The radiation condition requires that Φ_j behave at infinity like a radially outgoing wave and imposes a uniqueness which would not otherwise be present.

Substituting the expression for Φ, the above equations become

i) $$\nabla^2 \phi_j - (k \sin)^2 \phi_j = \emptyset$$

ii) $$\partial \phi_j / \partial Y - \upsilon \phi_j = \emptyset \qquad \upsilon = w^2/g$$

iii) $$\nabla \phi_j \cdot \mathbf{n} = v_n$$

iv) $$\partial \phi_j / \partial y = \emptyset$$

v) $$x \{\partial \phi_j / \partial x + ik\phi_j\} = \emptyset$$

where $\phi_j = \phi_j(x,y)$

Generally the analysis is carried out for $X_{j\emptyset} = 1$, thus giving the potentials associated with a unit amplitude motion. Condition (iii) can then be described as,

$$\partial \phi_1 / \partial n = -iwn_x$$

$$\partial \phi_2 / \partial n = -iwn_y$$

$$\partial \phi_3 / \partial n = -iw[xn_y - yn_x]$$

where $\mathbf{n}$ is the unit normal out of the body surface.

(b) Diffraction

Indicating the incident and diffracted wave potentials (for a regular wave) by $\Phi_\emptyset$ and Φ_4,

$$\Phi_j = \phi_j(x,y)\ \exp[i(zk\mathrm{Sin}\theta - wt)] \qquad j = \emptyset, 4$$

ϕ_4 too has to satisfy the set of equations (i) through (v) except for the fact that equation (iii) should now be;

$$(\partial/\partial n)(\phi_\emptyset + \phi_4) = \emptyset \quad \text{or,}$$

$$\partial\phi_4/\partial n = -\partial\phi_\emptyset/\partial n$$

Also,

$$\phi_\emptyset = -i\ (g\eta/\omega)\ \{\mathrm{Cosh}[k(h+y)]\ /\ \mathrm{Cosh}(kh)\}\ \exp[i(kx\mathrm{Cos}\theta)]$$

The linearized Bernoulli equation gives the pressure by $P(t) = -\rho\partial\Phi/\partial t$, giving the spatial pressures p_j and $p_{\emptyset 4}$ as,

$$p_j = \rho w i \phi_j$$

$$p_{\emptyset 4} = \rho w i (\phi_\emptyset + \phi_4)$$

Forces and moments caused by the dynamic pressure are

$$f_{ij}(w) = -\int p_j\ n_i\ ds \qquad i,j = 1,2,3$$

$$f_i(w,\theta) = -\int p_{\emptyset 4} n_i\ ds \qquad i = 1,2,3$$

where $n_1 = n_x$ $n_2 = n_y$ $n_3 = x n_y - y n_x$. $f_i(w,\theta)$ is the transfer function that converts wave information to a force for a given θ, w, for a stationary structure. This is also called the fluid exciting force. f_{ij} can be further broken in to parts proportional to acceleration and velocity, giving hydrodynamic mass and damping coefficients. This is done only for algebraic convenience in solving the equation of motion.

Hydrodynamic mass coeff. $a_{ij}(w) = -(\mathrm{Re}(f_{ij})\ /\ w\ )\ C_1$

Hydrodynamic damping coeff. $c_{ij}(w) = -(Im(f_{ij}))\ C_2$

C_1 and C_2 are nondimensionalising factors

$C_1 = 1 / \rho A$ sway, heave

$= 1 / \rho AB$ sway/roll

$= 1 / \rho AB^2$ roll

and $C_2 = w\ (B/2g)^{1/2} * C_1$

Non dimensional force coefficient $q_i = Abs(f_i) * C_3$

Phase $= Tan^{-1}[Im\ f_i / Re\ f_i]$

and $C_3 = 1 / \rho gAk\eta$ sway

$= 1 / \rho gB\eta$ heave

$= 1 / \rho g(B^3/12)\eta$ roll

η = incident wave amplitude

Numerical procedures to solve the above have been published by various authors (Garrison [17], Sayer and Ursell [53], Bai [3] and Yeung [4], Nafzger and Chakrabarti [42], Green [22], Georgeardis [20]). Vugts [63] did extensive experimental studies to compare hydrodynamic coefficients obtained by potential flow solutions with experimental results, for various cross sectional shapes (including rectangular cross section). The agreement was close.

3.3 Solution Procedure

Though integral equation methods seems to be the most tractable and efficient method, finite element method too has been used succesfully. A computer program was developed to solve for the complex velocity potential using integral equation method and Green's function technique. Incident and scattered wave

potentials were saved for later use in the drift force computations. The solution procedure is described below briefly.

Using the Green's identity, the potential $\phi = \phi(x,y)$ at any point on a smooth control surface boundary in the flow field can be written as,

$$(1/2)\,\phi(x,y) = -\int_{\Gamma} \phi(a,b)(\partial/\partial n)G(x,y:a,b) - G(x,y:a,b)(\partial/\partial n)\phi(a,b)\, d\Gamma(a,b)$$

where (x,y) and (a,b) are two points on the boundary Γ. $G(x,y:a,b)$ is the Green's function that has properties similar to the velocity potential which also satisfies the same boundary conditions as the veloity potential. Such Green's functions have been published by several authors including Wehausen and Laitone [64]. The numerical solution procedure involves discretization of the boundary and solving for the velocity potentials at the mid point of each element by applying the boundary conditions. The following set of linear equations will then result:

$$(1/2)\,\phi_i(x_i,y_i) - \sum_{j=1}^{N} \phi(a_j,b_j)(\partial/\partial n)G(x_i,y_i:a_j,b_j)(\Delta\Gamma)_j$$

$$= \sum_{j=1}^{N} G(x_i,y_i:a_j,b_j)(\partial/\partial n)\phi(a_j,b_j)(\Delta\Gamma)_j \,.$$

Numerical singularities occur when i=j, but methods are available to avert this difficulty (see for example Garrison [18]).

Two approaches to the problem are possible;

a) Use of a Green's function that satisfies all the boundary conditions except on the structure boundary. As a consequence the above equation has to be satisfied only on the structure boundary to solve for the velocity potential. In a typical numerical computation, this means the number of boundary elements as well as numerical errors associated with the discretization process and computer memory requirements are drastically reduced. One major disadvantage exists. That is the highly complicated nature of the Green's function which consumes large computer time.

b) On the other hand, use of a simple Green's function which satisfies only the Laplace equation takes only a fraction of the time required by more complicated function for computations. But the boundary conditions will now have to be satisfied on all the boundaries. This can introduce additional numerical errors too.

The following procedure was found to give optimum performance for the symmetric breakwater pontoon within the computer memory limitations.

(i) Choice (a) to compute hydrodynamic mass and damping

(ii) Choice (b) to compute direction dependent force coefficients

Some results for the West Point floating breakwater pontoon are shown in Tables 1, 2 and 3.

CHAPTER 4

Dynamic Response of the Structure

4.1 Finite Element Formulation

The coordinate system used is shown in the figure shown below. x and y axes are also the centeroidal axes of symmetry of the section.

Of the three degrees of freedom sway, heave and roll, heave motion is independent of the other two provided mooring configuration is symmetric about y-z plane. Sway and roll motions are coupled due to the partial submergence of the structure and the coupling caused by mooring. Computer memory requirements can therefore be minimized by considering heave and sway/roll motions separately, but at the cost of reducing the efficiency (and speed) of computation.

(a) Discretization of the Structure and Definition of Element Degrees of Freedom

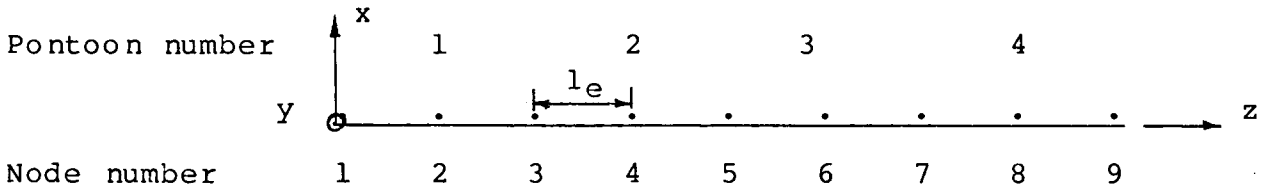

Plan view of a typical discretization of a 4 pontoon structure

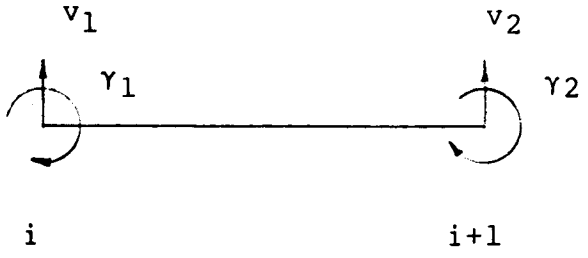

Heave
(Vertical Plane)

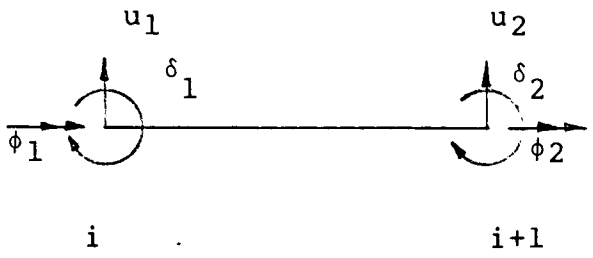

Sway/roll
(Horizontal Plane)

v=Vertical displacement

γ = Rotation in the vertical plane

u=Horizontal displacement

δ = Rotation in the horiz. plane

ϕ = Torsionaldisplacement about element axis

(b) Finite Element Analysis

Following the procedures outlined by Zeinkiewicz [66], the following element quantities can be computed,

Hydrodynamic mass $\mathbf{A}^e = \int_{l_e} \mathbf{N}^T \mathbf{a(w)} \mathbf{N}\, dl$

Hydrodynamic damping $\mathbf{C}^e = \int_{l_e} \mathbf{N}^T \mathbf{c(w)} \mathbf{N}\, dl$

Hydrodynamic buoyancy stiffness,

$$\mathbf{K'}^e = \int_{l_e} \mathbf{N}^T \mathbf{k'} \mathbf{N}\, dl$$

where, $\mathbf{a(w)}$, $\mathbf{c(w)}$, $\mathbf{k'}$ are sectional hydrodynamic mass, damping and buoyancy stiffness respectively. $\mathbf{N}$ is the interpolation matrix which gives the displacement at any point on the element in terms of nodal displacements,

$$\mathbf{u}(l) = \mathbf{N}\, \mathbf{u'}$$

where

$\mathbf{u}(1) = \{v(1) \ \gamma(1)\}^T$ and $\mathbf{u}' = \{ v_1 \quad \gamma_1 \quad v_2 \quad \gamma_2 \}^T$ for heave and

$\mathbf{u}(1) = \{u(1) \quad \delta(1) \quad \phi(1)\}^T$ and

$\mathbf{u}' = \{u_1 \quad \delta_1 \quad u_2 \quad \delta_2 \quad \phi_1 \quad \phi_2\}^T$ for sway/roll.

For heave, a(w), c(w), k' become scalars a_{yy}, c_{yy}, k'_{yy} $(= \rho B)$

For sway/roll,

$$\mathbf{a}(w) = \begin{bmatrix} a_{xx}(w) & a_{x\phi}(w) \\ a_{\phi x}(w) & a_{\phi\phi}(w) \end{bmatrix}$$

$$\mathbf{c}(w) = \begin{bmatrix} c_{xx}(w) & c_{x\phi}(w) \\ c_{\phi x}(w) & c_{\phi\phi}(w) \end{bmatrix}$$

$$\mathbf{k}' = \begin{bmatrix} \emptyset & \emptyset \\ \emptyset & k_{\phi\phi} \end{bmatrix}$$

Also,

$$k_{\phi\phi} = \rho g A H_m$$

where H_m is the distance between the meta center and the center of gravity of the section.

(c) Choice of Interpolation Matrix **N**

Choice of the interpolation matrix **N** is an important decision that has to be made in a finite element analysis. A knowledge of actual behavior of the structure and experience in finite element analysis is helpful for optimum numerical performance. It is common in standard structural analysis to

describe displacements associated with flexural bending along the structure with a third order polynomial and torsional displacements with a linear function (see for example McGuire and Gallagher [37]). On other hand using cubic polynomials in the computation of hydrodynamic force spectral matrix will drastically increase computation time. Use of a linear function to compute the force matrix will make the procedure "inconsistent" with the rest, but the error introduced in this case is negligible for long slender structures (oral conversation with Hartz). Following this approach, the displacement at any point on the element can be expressed as,

Heave:

$$[v \ \gamma \ ]^T = \begin{bmatrix} N_1 & N_2 & N_3 & N_4 \\ N_1' & N_2' & N_3' & N_4' \end{bmatrix} [v_1 \quad \gamma_1 \quad v_2 \quad \gamma_2]^T$$

Sway/Roll:

$$[u \ \delta \ \phi]^T = \begin{bmatrix} N_1 & N_2 & N_3 & N_4 & \emptyset & \emptyset \\ N_1' & N_2' & N_3' & N_4' & \emptyset & \emptyset \\ \emptyset & \emptyset & \emptyset & \emptyset & N_5 & N_6 \end{bmatrix} [u_1 \ \delta_1 \ u_2 \ \delta_2 \ \phi_1 \ \phi_2]^T$$

where,

$$N_1 = 1 - 3(1/l_e)^2 + 2(1/l_e)^3$$

$$N_2 = -l(1 - 1/l_e)^2$$

$$N_3 = 3(1/l_e)^2 - 2(1/l_e)^3$$

$$N_4 = -l[(1/l_e)^2 - 1/l_e]$$

$$N_5 = 1 - 1/l_e$$

$$N_6 = 1/l_e$$

$$N_i' = -(d/dl)N_i \qquad i = 1,\ldots 4$$

For hydrodynamic force computations $N_2 = N_4 = \emptyset$ and N_1, N_3 are

replaced by N_5 and N_6 respectively to give a linear interpolation polynomial. Rows that represent degrees of freedom not hydrodynamically loaded can be deleted to reduce computation.

Now, the hydrodynamic mass, damping and buoyancy stiffness matrices for the whole structure can be obtained by summing $\mathbf{A}^e$, $\mathbf{C}^e$ and $\mathbf{K'}^e$ respectively, to obtain $\mathbf{A}$, $\mathbf{C}$ and $\mathbf{K'}$.

The complex transfer function vector which relates the wave amplitude to the sectional force $\mathbf{f}(\theta,w)$ was earlier derived.

$$\mathbf{f}(\theta,w) = [\, f_u(\theta,w) \quad f_\phi(\theta,w)\,]^T \quad \text{for sway/roll}$$

$$= f_v(\theta,w) \quad \text{for heave}$$

The stochastic time dependent force can then be given by [15],

$$f(t) = \int_{-\infty}^{\infty} \mathbf{f}(\theta,w)\, \exp[i(kz\mathrm{Sin}\theta - wt)]\, dZ_\eta(\theta,w)$$

where $Z_\eta(\theta,w)$ is the spectral process associated with the wave amplitude (assumed stationary) with orthogonal increments. Using the same interpolation functions defined above, the force vector on the i th element is given by,

$$\mathbf{f}_i(t) = \int_{l_i}\int_{-\infty}^{\infty} \mathbf{N}^T \mathbf{f}(\theta,w)\, \exp[i(kz_i\mathrm{Sin}\theta - wt)]\, dZ_\eta(\theta,w)\, dl_i$$

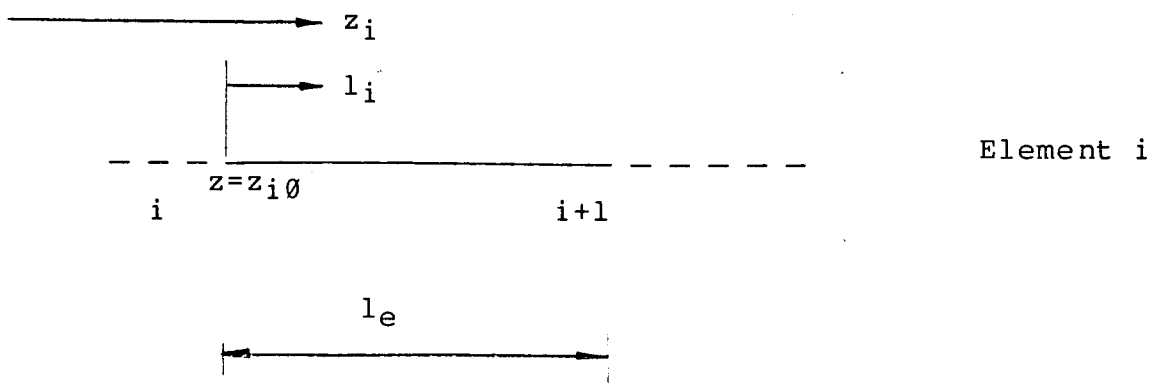

Note that $Z_i = Z_{i\emptyset} + l_i$

where $Z_{i\emptyset}$ is the length from the origin to the first node of the i th element (see figure above).

It can be shown that the spectral matrix of the forces between elements i and j is given by (see Appendix B for proof)

$$\mathbf{S_{fi,j}(w)} = \int_\theta \left[\int_{l_1}\int_{l_2} \mathbf{N_i}^T \mathbf{f}(\theta,w)\mathbf{f}(\theta,w)^{*T} \mathbf{N_j} \exp\{i[k(z_i-z_j)\sin\theta\} \right.$$

$$\left. dl_1 dl_2 \right] S_\eta(\theta,w)\, d\theta$$

where, $Z_i = Z_{i\emptyset} + l_i$

$Z_j = Z_{j\emptyset} + l_j$

If the directional spread function is defined as $\Psi(\theta) = S_\eta(\theta,w) / S_\eta(w)$ then the above relation becomes,

$$\mathbf{S}_{f\ i,j}(w) = \mathbf{G_{ij}}(w)\ S_\eta(w)$$

where $\mathbf{G}_{ij}(w) = \int_\theta \left[\int_{l_i}\int_{l_j} \mathbf{N}_i^T \mathbf{f}(\theta,w)\mathbf{f}(\theta,w)^{*\ T} \mathbf{N}_j \exp\{i[k(z_i-z_j)\sin\theta\} \right.$

$$\left. dl_i dl_2 \right] \Psi(\theta)\, d\theta$$

$$= \int_\theta \left[\int_{l_i}\int_{l_j} \mathbf{N}_i^T \mathbf{f}(\theta,w)\mathbf{f}(\theta,w)^{*\ T} \mathbf{N}_j \exp\{i\sin\theta[(z_{ij} + (l_i-l_j)]\} \right.$$

$$\left. dl_i\, dl_j \right] \Psi(\theta)\, d\theta$$

where $z_{ij} = z_{i\emptyset} - z_{j\emptyset}$

Summing over all the elements for the whole structure gives the Spectral matrix,

$$\mathbf{S_F}(w) = \sum_{i,j} \mathbf{S_{f\ i,j}}(w)$$

$$= \sum_{i,j} \mathbf{G}_{ij}(w)\ S_\eta(w)$$

$$= \mathbf{G}(w)\ S_\eta(w)$$

where $$G(w) = \sum_{i,j} G_{ij}(w)$$

4.2 Mooring Analysis

The effect of mooring on the structure is an important parameter that determines the response of a floating structure, especially in sway and to a smaller extent in roll. In most cases its effect on heave is relatively small due to the dominant buoyancy stiffness except in the special case when the slack in the cable is zero. In addition the presence of mooring contributes to the hydrodynamic coupling between sway and roll motions. Therefore, the accurate determination of mooring constants is essential in dynamic response analysis.

Adee [1] developed a rigorous mooring analysis program for his breakwater study. This was considered adequate for the present study. The theory, which is found in his report in detail, is summarized below.

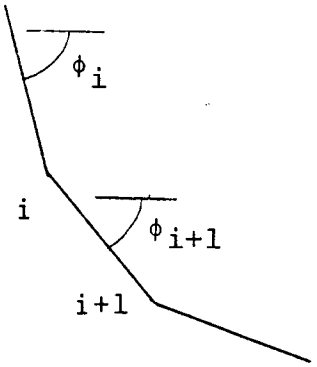

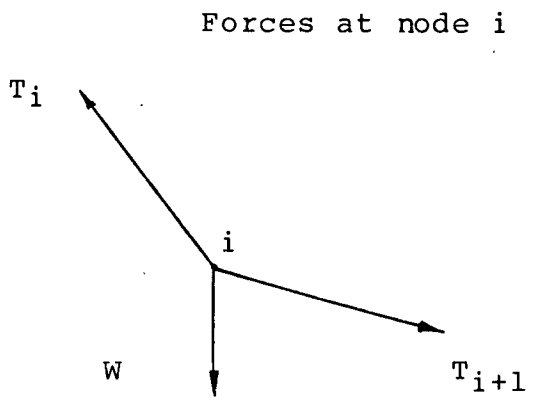

The figure above shows a section of the anchor cable near nodes i and i+1. The weight of each cable section is considered to be concentrated at the bottom of the section. In order to find the shape of the cable, summations of forces are computed for static equilibrium at each node, giving

$$\phi_{i+1} = \mathrm{Tan}^{-1}\left[\frac{T_i \sin\phi_i - W_i}{T_i \cos\phi_i}\right]$$

where T_i = tension in segment i

W_i = weight of section i concentrated at node i

i = angle between element i and horizontal

The new angle is then used to compute the tension in the next section,

$$T_{i+1} = \frac{T_i \cos\phi_i}{\cos\phi_{i+1}}$$

The computation begins at the free surface so that at any node the tension in the cable section above as well as the angle of that section to the horizontal is known.

Coordinates of each node are computed by,

$$x_{i+1} = x_i + l_{ext\ i+1} \cos\phi_{i+1}$$

$$y_{i+1} = y_i + l_{ext\ i+1} \sin\phi_{i+1}$$

where l_{ext} is the length of element under tension.

At the last node the y coordinate is compared with the depth of the anchor. If there is a difference, the initial tension value is adjusted (which is guessed). From then on the procedure is repeated over as many iterations as needed adjusting the

tension until the depth is accurate to within Ø.Ø1% . Among the ouput are the stiffness of the cable in vertical and horizontal directions.

4.3 Frequency Response Solution

The equation of motion is

$$(\mathbf{M} + \mathbf{A})\ddot{\mathbf{r}} + \mathbf{C}\dot{\mathbf{r}} + (\mathbf{K} + \mathbf{K}')\mathbf{r} = \mathbf{F}$$

where **M** and **K** are structural mass and stiffness matrices and **A**, **C** and **K'** are hydrodynamic mass damping and stiffnes matrices as described previously. The structural damping has been assumed neglegible.

Substituting $\mathbf{r} = \mathbf{r}_{\emptyset} \exp(-iwt)$, $\mathbf{F} = \mathbf{F}_{\emptyset} \exp(-iwt)$ fourier transforming and squaring the above equation gives

$$S_{\mathbf{r}}(w) = \mathbf{H}(w)\ S_{\mathbf{F}}(w)\ \mathbf{H}^{*T}(w)$$

where $\mathbf{H}(w) = [-w^2(\mathbf{M} + \mathbf{A}(w)) - iw\mathbf{C}(w) + (\mathbf{K} + \mathbf{k}')]^{-1}$.

$S_{\mathbf{F}}(w)$ was derived in the previous section and is given by $G(w) * S_{\eta}(w)$.

Then,

$$S_{\mathbf{r}}(w) = \mathbf{R}(w)\ S_{\eta}(w)$$

where $\mathbf{R}(w) = [\mathbf{H}(w)\ \mathbf{G}(w)\ \mathbf{H}^{*T}(w)]$ is the response transfer function of the breakwater.

CHAPTER 5

Non Linearities

The above derivations based upon classical linear spectral techniques become increasingly less applicable when non linearities dominate. For a moored floating structure there are two major hydrodynamically non-linear situations that must be considered in the analysis (Structural non-linearities, such as non-linear behavior of mooring cables, will not be considered).

i) Non linear viscous damping dominates in roll near the resonant frequency of the structure.

ii) Low frequency drift oscillations - This is the situation where the structure undergoes large amplitude rigid body drift oscillations at or near the undamped natural frequency of the mooring system. Large mooring forces will then result.

5.1 Viscous Roll Damping

Fig.8 shows the roll rigid motion of a rectangular cylinder as given by Vugts [63]. The dashed line shows the theoretical potential flow solution and the solid line shows the experimental measurement. It can be seen that the error introduced by not considering the viscous contribution causes a significant error at and near the resonant frequency. In the West Point breakwater, the roll resonance frequency is about .3 hz, (Miller [39]) which is also close to the peak spectral

frequency, which helps to further magnify the problem.

Various authors (for example Salvesen [51], Schmitke [54]) have suggested ways of introducing the contribution from viscous roll damping. The disadvantage is that almost all of them use an iterative procedure in the solution of the equation of motion due to the fact that the damping coefficient is a function of square of roll amplitude. Such a procedure, if used in the type of computation described previously in this report, will consume an enormous amount of computer time making the whole exercise impractical. For this work therefore the model will be calibrated using field data. Some method of generalizing the results will be sought.

5.2 Drift Forces

Previously, the wave-excited forces on the structure were derived using the linear potential theory. A more thorough evaluation of hydrodynamic forces requires one to consider higher order contributions to the wave induced force. This second order contribution leads to a drift force that consists of a mean component and a low frequency oscillating component. Though small in magnitude, this can cause the breakwater to undergo large amplitude drift oscillations at or near the undamped natural frequency of the mooring system. Computationally, difficulties arise since instantaneous water surface and second-order potential have to be considered. In this study, the viscous contribution is ignored and only the potential flow

solution is considered. This means that the breakwater has to be "large" compared to the wave length, which in most cases is true.

(a) Previous Work

Pinkster [46,48], and Standing [57,58] predicted second order forces on barges and ships and Faltinsen and Loken [16] computed second order forces on two dimensional infinite cylinders. Beam seas were assumed in both cases. Dalzell [13], Pinkster [48] and later Miksad, Powers, Kim, Jones, Solis and Fischer [40] applied cross - bispectral techniques to measured incident waves and structure motions to obtain a quadratic drift force transfer function.

In the following a theoretical model is developed to predict second order force and response spectra for a floating breakwater in a directional sea. As will be noted, the computational effort will be roughly squared when considering directional seas as compared to the case of beam seas. The low frequency forces are critical only for the rigid motion of the breakwater as this is the case where the low natural frequency of the mooring system dominates. The flexural low frequency displacements will be almost nonexistent. Therefore the analysis will be confined to one of rigid body type.

(b) Theoretical Model

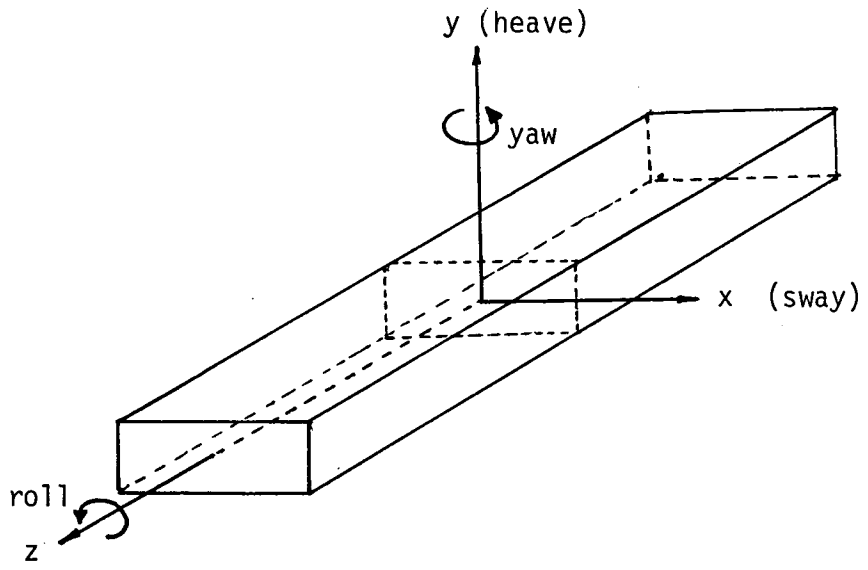

In the following derivation, subscripts Ø,1,2 represent zeroth, first and second order terms.

Let $S(x,y) = S_{\emptyset}(x_{\emptyset},y_{\emptyset}) + S_1(x_1,y_1)$

where S is the instantaneous wetted boundary at a given cross section, $S_{\emptyset}$ is the mean wetted boundary and S_1 the immersion of the structure as a consequence of wave and structure motion.

The fluid dynamic force (per unit length) on the structure is given by,

$$f = -\int_S p\, n\, ds$$

where n is the instantaneous normal to the surface given by

$$n = n_{\emptyset} + \epsilon n_1$$

$n_\emptyset$ = normal vector to surface S (= $[\ n_{x\emptyset}\ n_{y\emptyset}]^T$).

εn_1 = change of normal vector arising from the motion of the structure.

ε = a small factor << 1

The vector n_1 is given by

$$n_1 = R_1\ n_\emptyset$$

where R_1 is matrix consisting of first order rotation at the cross-section considered. The linear and non-linear pressure is given by

$$p = -\rho gy - \rho\Phi_t - (1/2)\ \rho(\nabla\Phi)^2$$

where Φ and p are given by,

$$\Phi = \varepsilon\Phi_1 + \varepsilon^2\Phi_2$$

$$p = p_\emptyset + \varepsilon p_1 + \varepsilon^2 p_2$$

$p_\emptyset$ = hydrostatic pressure = $-\rho gy$

p_1 = first order pressure = $-\rho gy_1 - \rho\partial\Phi_1/\partial t$

p_2 = second order pressure = $-(1/2)\ \rho(\nabla\Phi_1)^2 - \rho\partial\Phi_2/\partial t - \rho(\mathbf{s}_1\cdot\nabla\partial\Phi_1/\partial t)$

$\mathbf{s}_1 = [x_1\ y_1]$ is the displacement of the center of gravity of the section. (See Appendix C for derivation of p_2).

Also,

$$\mathbf{f} = \mathbf{f}_\emptyset + \varepsilon\mathbf{f}_1 + \varepsilon^2\mathbf{f}_2$$

Substituting in the expression for **f**,

$$\mathbf{f}_\emptyset + \mathbf{f}_1 + \varepsilon^2\mathbf{f}_2 = \int_{S_\emptyset+S_1}(p_\emptyset + \varepsilon p_1 + \varepsilon^2 p_2)(\mathbf{n}_\emptyset + \varepsilon\mathbf{n}_1)\ dS$$

Extracting zeroth, first and second order terms,

$$\mathbf{f}_\emptyset = \rho g \int_{S_\emptyset} y\mathbf{n}\ ds = \rho gA\mathbf{k}$$

$$\mathbf{f}_1 = \int_{S_\emptyset} \rho g y_1 \mathbf{n}_\emptyset \, dS + \int_{S_\emptyset} \rho \partial \Phi_1 / \partial t \, \mathbf{n}_\emptyset \, dS$$

The first term is easily recognized as the hydrodynamic restoring force.

The second order force which produces the "drift" force is given by,

$$\mathbf{f}_2 = -\int_{S_\emptyset} p_1 \, \mathbf{n}_1 \, dS - \int_{S_\emptyset} p_2 \, \mathbf{n}_\emptyset \, dS - \int_{S_1} p_1 \mathbf{n}_\emptyset dS$$

The first integral $= -\int_{S_\emptyset} p_1 \mathbf{n}_1 \, ds = -R_1 \int_{S_\emptyset} p_1 \mathbf{n}_\emptyset \, ds = R_1 \mathbf{f}_1$

$= R_1 m \ddot{s}_1$ by Newton's law

The second integral is obtained by directly substituting for p_2.

Using $p_1 = -\rho g y_1 - \rho \partial \Phi_1 / \partial t = -g y_1 + \rho g \eta_1$

where η_1 is the wave amplitude,

The third integral $= -\int_{S_1} p_1 \mathbf{n}_\emptyset \, dS = -\int_{y_{1WL}}^{y_1} (-\rho g y_1 + \rho g \eta_1) \mathbf{n}_\emptyset \, dy$

where y_{1WL} is the vertical displacement of the mean water level of the structure.

The above, as can be seen, is the integration of the pressure from actual mean water surface to the wave crest (or trough). This length is small enough to approximate the pressure by a hydrostatic distribution. Therefore,

$$\text{third term} = -(1/2)\rho g \eta_{1r}^2 \mathbf{n}_\emptyset$$

where $\eta_{1r} = \eta_1 - y_{1WL}$ is the relative wave amplitude.

The second order force then reduces to,

$$\mathbf{f}_2 = -(1/2)\rho g \eta_{1r}^2 \mathbf{n}_\emptyset + \mathbf{R}_1 \mathbf{m} \ddot{\mathbf{s}}_1 + \int_{S_\emptyset} (1/2)\rho(\nabla\Phi_1)^2 \mathbf{n}_\emptyset \, dS$$

(i) (ii) (iii)

$$+ \int_{S_\emptyset} \rho \partial\Phi_2/\partial t \, \mathbf{n}_\emptyset \, dS + \int_{S_\emptyset} \rho(\mathbf{s}_1 . \nabla \partial\Phi_1/\partial t) \mathbf{n}_\emptyset \, dS$$

(iv) (v)

Note that the above expression gives the second order force per unit length at a given section. m is the mass per unit length. Also note that the first term should be computed on both vertical walls and the difference should be considered as the contribution due to relative wave height.

Assuming that variation of the force between two nodes is linear, the total force (and the moment) can be obtained by integration along the length of the structure. Thus,

$$\mathbf{F}_2 = \int_L \mathbf{f}_2 \, dl$$

$$\mathbf{M}_2 = \int_L \mathbf{x} \times \mathbf{f}_2 \, dl$$

(c) Numerical considerations

In considering low frequency motions of floating breakwaters, knowledge of their physical behavior can be utilized to simplify the theoretical model. Firstly, low frequency motions are significant only in sway and to a lesser extent in yaw. But in general, to solve for either sway or yaw, roll motion too has to be considered since all three motions are coupled with each other. If the coordinate system origin is

chosen at the mid point, added mass and damping terms in yaw becomes uncoupled from the rest due to symmetry. If the mooring cable lay-out is symmetric about the x-y plane (which is usually the case), the yaw motion becomes completely independent of sway and roll. For a typical floating breakwater the second order roll oscillation is neglegible although this may not be true for a large vessel. Therefore, second order roll motion will be neglected in this model. Later by numerical computation it will be shown that term (i) dominates the mean drift force, while term (iii) helps to reduce its effect. This is in contrast to the practice that considered only term (iii) to augment linear computations.

Derivation of the Quadratic Force Transfer Function

Careful examination of the terms involved in the expression for the second order force shows that each term is formed by the product of two first order terms. Let the two first order quantities be given by,

$$A = \sum_{n=1}^{N} n\_n A_n \, e^{-iw_n t} \text{ and}$$

$$B = \sum_{m=1}^{N} n\_m B_m \, e^{-iw_m t}$$

where n (and m) represents a wave with a given frquency and direction. Note that A_n and B_m are complex and contain the phase information including those due to wave number and position

variations. Keeping in mind that only the real part is of interest, the low frequency portion of the product of A and B is given by [58],

$$AB = (1/2) \sum_{n=1}^{N} \sum_{m=1}^{N} \eta_n \eta_m A_n B_m^* \, e^{-i(w_n - w_m)t}$$

If we combine the $w_n - w_m$ and $w_m - w_n$ terms, the resulting coefficients F_{nm} will have a symmetric real part and an anti-symmetric imaginary part, i.e $F_{nm} = F_{mn}^*$. Obtaining the results in this form reduces the computational effort as well as data storage requirements. If the second order force is written as

$$F_2 = \sum_{n=1}^{N} \sum_{m=1}^{N} \eta_n \eta_m F_{nm} \, e^{-i(w_n - w_m)t}$$

then, it can be shown that [58],

$$F_{nm} = (A_n B_m^* + A_m^* B_n) / 4$$

F_{nm} is called the **Quadratic Force Transfer Function** for the pair of waves denoted by subscripts n and m.

To elaborate the above procedure, contribution to term (iii) from the incident and diffraction potentials are computed below. The procedure is similar for other terms although the undelying steps may not be explicitly obvious for some terms.

$$\text{Term (iii)} = \int_{S\emptyset} (1/2) \rho (\nabla \Phi_1)^2 \, \mathbf{n}_\emptyset \, dS$$

It was earlier shown that the first order diffraction + incident velocity potential can be written in the form

$$\Phi_1 = \phi_1(x,y) \, e^{i(kz\sin\theta - wt)}$$

$$\partial\Phi_1/\partial x = \phi_{1x}(x,y)\, e^{i(kz\mathrm{Sin}\theta - wt)}$$

$$\partial\Phi_1/\partial Y = \phi_{1y}(x,y)\, e^{i(kz\mathrm{Sin}\theta - wt)}$$

$$\partial\Phi_1/\partial z = (ik\mathrm{Sin}\,)\phi_1(x,y)\, e^{i(kz\mathrm{Sin}\theta - wt)}$$

where, $\phi_{1x} = \partial\phi_1/\partial x$

$\phi_{1y} = \partial\phi_1/\partial Y$

It is then easy to see that low frequency contribution to term (iii) from these two potentials is of the form

$$\sum_{n=1}^{N}\sum_{m=1}^{N} \eta_n \eta_m \, t_{nm} \, e^{i[(\varepsilon_n - \varepsilon_m) - (w_n - w_m)]}$$

where n and m denote two wave fronts with frequency and direction w_n, θ_n and w_m, θ_m respectively and

$$t_{nm} = (1/2)\int_{S\emptyset}[(1/2)\mathbf{A}_n\mathbf{A}_m^{*T}\,\mathbf{n}_\emptyset]\, dS_\emptyset$$

A_j is given by

$$\mathbf{A}_j = \{\phi_{1x}\ \phi_{1y}\ \ ik_j\ \phi_1 \mathrm{Sin}\theta_j\}\, e^{ikz\mathrm{Sin}\theta j} \ /\ \eta_j$$

As described previously, we can combine $w_n - w_m$ and $w_m - w_n$ terms to obtain the contribution to the quadratic force transfer function given by

$$f_{nm} = (1/8)\int_{S\emptyset}[A_n A_m^{*T} + A_m^{*} A_n^{T}]\, \mathbf{n}_\emptyset\, dS_\emptyset$$

Note that above expression gives the transfer function at the cross-section considered. The complete transfer function has to be then obtained by integrating the above along the water line.

The only other term that needs special attention is term (iv) as this term consists of the second order potential. In computing term (iv) it is assumed that the second order wave is undisturbed due to second order diffraction and motions of the

structure. An expression for the undisturbed second order potential is given in [58],

$$\Phi_2 = -i \sum_{n=1}^{N-1} \sum_{m=1}^{N+1} \eta_n \eta_m C_{nm} \mathrm{Cosh}[K_{nm}(h+y)] \exp\{i[K_{nm} x \mathrm{Cos}\theta_{nm} + K_{nm} z \mathrm{Sin}\theta_{nm} - (w_n - w_m)t + \varepsilon_n - \varepsilon_m]\}$$

where,

$$C_{nm} = (1/2)g^2 \{k_n^2 \mathrm{Sech}^2 k_n h/w_n - k_m^2 \mathrm{Sech}^2 k_m h/w_m + 2(w_n - w_m) k_n k_m [\mathrm{Cos}(\theta_n - \theta_m) + \mathrm{Tanh} k_n h \ \mathrm{Tanh} k_m h]\} / \{K_{nm} g \mathrm{Sinh} K_{nm} h - (w_n - w_m)^2 \mathrm{Cosh} K_{nm} h\} \quad \text{and}$$

$$K_{nm} \mathrm{Cos}\theta_{nm} = k_n \mathrm{Cos}\theta_n - k_m \mathrm{Cos}\theta_m$$

$$K_{nm} \mathrm{Sin}\theta_{nm} = k_n \mathrm{Sin}\theta_n - k_m \mathrm{Sin}\theta_m$$

It is easy to see that the integration of $\rho \partial \phi_2 / \partial t$ over the cross section results in a contribution to the quadratic transfer function similar in form to the one derived for term (iii).

(d) Drift Force and Response Spectra

Let us denote the quadratic force transfer function (for either sway or yaw) by, $F_{nm} = F(w_n, \theta_n; w_m, \theta_m)$ for each frequency/direction pair. From the theory of spectral superposition, it can be shown that the mean drift force is given by,

$$F_{2\ \mathrm{mean}}(\psi_i) = \int_w \int_\theta \sqrt{S(w,\theta) S(w, \theta+\psi_i)}\, |F(w,\theta; w, \theta+\psi_i)|\, dw d\theta$$

The total mean force is the sum of those for all difference directions. Or,

$$F_{2\ mean} = \sum_i F_{2\ mean}(\psi_i)$$

The spectral density matrix of the low frequency drift oscillation force is given by

$$S_{F2}(\mu,\psi) = \int_\theta \int_\omega S_\eta(w+\mu,\theta+\psi)\ S_\eta(w,\theta)\ |F(w,\theta;w+\mu,\theta+\psi)|^2\ d\theta dw$$

where μ and ψ are difference frequency and direction respectively. The difference direction can be conveniently integrated out to obtain

$$S_{F2}(\mu) = \int_\psi S_{F2}(\mu,\psi)\ d\psi$$

The low frequency response spectral matrix can be obtained by,

$$S_{r2} = H(w)H(w)^* S_{F2}$$

where H(w) is the frequency response function given by

$$H(w) = 1 / [-w^2(M+A(w)) - iwC(w) + (K+k')]$$

Note that H(w) is a scalar since only one motion degree of freedom is considered at a time.

CHAPTER 6

Further Considerations

6.1 Time Domain Solution

The above non linear properties can be easily included in time domain integration technique. In this case, the frequency dependent hydrodynamic quantities will have to be converted in to the time domain by the relation

$$\mathbf{A}(t) = \int_{-\infty}^{\infty} \mathbf{A}(w)\ \exp(iwt)\ dw$$

$$\mathbf{C}(t) = \int_{-\infty}^{\infty} \mathbf{C}(w)\ \exp(iwt)\ dw$$

In a real situation the above computation becomes cumbersome and time consuming. In most cases therefore **A** and **C** are assumed constant, equal to their values at the peak spectral frequency.

6.2 Curved Structures

The above developments, as can be seen, are valid for a straight breakwater only. As a computer memory saving measure, the global and element coordinate system were made to coincide, though it was not explicitly mentioned. In the case of a curved breakwater (for example one consisting of two straight "legs"), assuming the loaded degrees of freedom still remain sway, heave and roll, the above model can be used with 2 minor changes

1. The relationship $\mathbf{u} = \mathbf{N}\ \mathbf{u}'$ has to be replaced by $\mathbf{u} = \mathbf{N}\ \mathbf{b}\ \mathbf{u}'$, where **b** is the connectivity matrix which converts element displacements to global displacements, which now is position dependent.

2. The wave heading angle θ will also now depend on the positioning of each element

CHAPTER 7

COMPARISON OF RESULTS WITH FIELD DATA

7.1 Computer Programs

Several computer programs had to be developed for the analysis described in the previous chapters. Function of each program and their reltionship to each other is shown in fig. 9 and summarized below.

Program name	Function
BWDIR	Computes directional wave spectra from the field wave records.
HCOF	Computes radiation velocity potentials (used by program DRIFT) and hydrodynamic mass and damping coefficients (used by program DYN)
HFORC	Computes diffraction velocity potentials (used by program DRIFT) and hydrodynamic forcing coefficients and their phases (used by program DYN)
DYN	Dynamic (first order, "high" frequency) analysis of the structure. Gives spectral information of hydrodynamic force, structure response and internal structure force distribution along the structure. Response is used by program DRIFT.
DRIFT	Computes second order hydrodynamic drift forces (mean and oscillating) and resulting mean displacement and low-frequency oscillation of the structure. Mooring forces should be computed based on the results of this program. (At the time of writing DRIFT was nearing

completion)

All the programs were designed to run in a micro-computer with about 256k of memory.

7.2 Results and comparison with field data

Program DYN was used to analyze the West Point experimental prototype breakwater motion and the results were compared with field data. The wave field was simulated using the measured wave spectrum at the site (Fig. 1Ø). The structure was modelled using four finite elements as shown below. More elements are needed if higher numerical accuracy is required.

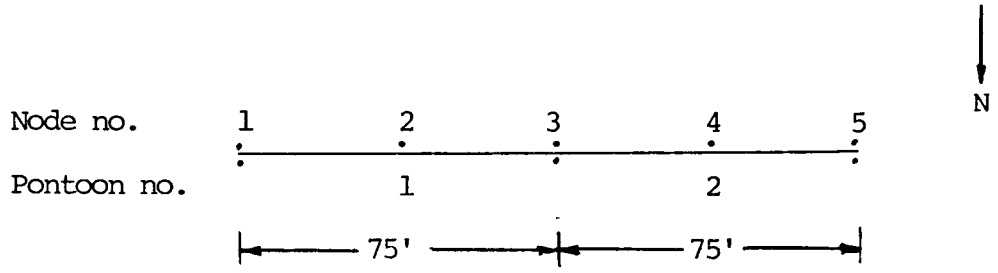

One of the assumptions in the theoretical model described in the preceding chapters is that the end effects of the structure are neglegible. In other words the length dimension of the structure must be much larger than the other dimensions. This is true in the case of a typical floating breakwater or a bridge. On the contrary, the West Point break water was considered a "short" structure because it had only two pontoons (each pontoon was 75' long, 16' wide and the draft was 3.5'). Inspite of the relative shortness of the structure, satisfactory agreement of predicted acceleraions with breakwater accellerometer readings show that

this assumption has not introduced any appreciable error.

Using program DYN, the spectral matrices of hydrodynamic force and the resulting structure response were computed. The responses are those at the centeroid of each section (node). Fig. 11 shows the hydrodynamic sway force auto spectrum at midpoint (node 3) of the structure and Figs. 12 and 13 show the coherence between the hydrodynamic sway force at midpoint and the hydrodynamic sway force along the rest of the structure for the frequencies Ø.2 hz and Ø.4 hz. Notice that the coherence falls off more rapidly as the frequency grows higher. Therefore if emperical relationships are used to model hydrodynamic force coherence one must take its frequency dependence in to account. In long structures we can expect to find the coherence going down to zero even at lower frequencies, if the two points under consideration are spaced far enough. The "effectiveness" of hydrodynamic force which induces the structural response in such cases is highly dependent on the coherence pattern. If we assume that the sea is uni-directional and assume a 2-d configuraton, we would then be implicitly assuming that the force coherence along the structure is unity and drastic over-estimation of structure response will then result. The sway response auto spectrum at midpoint as estimated by DYN is shown in figure 14.

Using interpolation functons described in Ch. 4 and standard coordinate transformations, the acceleration spectrum at the accelerometer locations were computed and compared with measured accelerometer readings. Fig. 16 shows the comparison of

predicted sway accelleration with that measured at the east pontoon. The agreement is very satisfactory as evidenced by the close variances.

Fig. 15 shows the autospectrum of the horizontal strucutre shear force computed by DYN. Moments are small as the structure is relatively short.

Similar results obtained for heave motion are shown in Figs. 17 through 22.

It is left for the designer to obtain design values from these results. A common practice is to use the variance of the process to find design values with a known probability of occurence. If structure fatigue is of interest the designer will be mainly interested in the so called "zero crossing period" of forces and moments, i.e the time between two consecutive points where the value of the process goes to zero.

REFERENCES

1. Adee , B.H., Richey, E.P. and Christensen, D.R. : Floating Breakwater Field Assesment Program, Friday Harbor, Washington, Technical Paper No. 76-17, U.S. Army Corps of Engineers, Coastal Engineering Rersearch Center, 1976

2. Baggeroer, A.B.: "Recent Signal Processing Advances in Spectral Estimation and their Application to Offshore Structures", Proc. of the Second International Conference on the Behavior of Off-Shore Structures, London, England, Aug 1979.

3. Bai, K.J. : "Diffraction of Oblique Waves by an Infinite Cylinder", Journal of Fluid Mechanics, Vol. 68, pp 513-535, 1975.

4. Bai, K.J. and Yeung, R.W.: "Numerical Solutions to Free Surface Flow Problems", Tenth Symposium of Naval Hydrodynamics, MIT, 1974.

5. Borgman, L.E.: "Statistical Models for Ocean Waves and Wave Forces", Advances in Hydroscience, edited by Ven Te Chow, Vol. 8, Academic Press, New York 1972.

6. Borgman, L.E.: "Ocean Wave Simulation for Engineering Design" , J. Waterways Harbors Div., ASCE, Vol. 95, No. WW4. 1969,pp 556-583.

7. Bretcschneider, C.I.: Topics in Ocean Engineering, Vol. 2, Gulf Publishing Company, 1970.

8. Capon, J., Greenfield, R.J. and Kolker, R.J.: "Multidimensional Maximum Likelihood Processing of a Large Aperture Seismic Array", Proceedings of the IEEE, Vol.55, Feb 1967.

9. Capon, J.: "High-Resolution Frequency-Wavenumber Spectrum Analysis", Proceedings of the IEEE, Vol. 57, No.8, Aug 1969.

10. Chapman, R. Bruce : "Survey of Numerical Solutions for Ship Free-Surface Problems", Second International Confrrence on Numerical Ship Hydrodynamics, Sep 1977.

11. Cronin, D.J. and Galgoul, N.S. : "Dynamic Analysis of Deep Water Platforms Using an Enhanced Modal Method", Proc. of the 3rd Int. Symposium on Offshore Engineering, Brazil, 1981 - Offshore Engineering, edited by Carneiro, Ferrante and Batista, Pentech

Press, London.

12. Courant, R. and Hilbert, D: Methods of Mathematical Physics, Vol.1, Interscience Publishers, New York, 1953.

13. Dalzell, J.: "Application of the Functional Polynomial Model to the Added Resistance Problem", 11 th Symposium on Naval Hydrodynamics, University College, London, 1976.

14. Davis, R.E. and Regier, L.A.: " Methods for Estimating Directional Wave Spectra from Multi-element Arrays, J. of Marine Research , Vol. 35, No.3, Aug 1977.

15. Doob, L: Stochastic Processes, Wiley, 1953.

16. Faltinsen, O.M. and Loken, A.E.: "Slow Drift Oscillations of a Ship in Irregular Waves", Applied Ocean Reasearch, vol. 1, pp. 21-31, 1979.

17. Garrison, C.J.: "Hydrodynamics of Large Objects in the Sea: Part 1 - Hydrodynamic Analysis", Journal of Hydronautics, Vol. 8, No. 1, 1974.

18. Garrison, C.J.: "Hydrodynamic Loading of Large Offshore Structures: Three Dimensional Source Distribution Methods ", Numerical Methods in Offshore Engineering, edited by O.C. Zienkiewicz, Wiley, 1976

19. Garrison, C.J.: "On the Interaction of an Infinite Shallow Draft Cylinder Oscillating at the Free Surface with a Train of oblique Waves", Journal of Fluid Mechanics, Vol. 39, part 2, pp. 227-255, 1969.

20. Georgiadis, C.: Wave Induced Vibrations of Floating Structures, Ph.D Dissertation, University of Washington, Seatle, 1981.

21. Geckinli, Nezih C. and Davras, Yavuz : Discrete Fourier Transformation and its Applications to Power Spectra Estimation, Studies in Electrical and Electronic Engineering, Pt 8, Elsevier Scientific Publishing Co., 1983.

22. Green, M.W. : " A Problem Connected with the Oblique Incidence of Surface Waves on an Immersed Cylinder", Journal of the Inst. of Math. and its Applications, Vol.82-98, 1971.

23. Hartz, B.J.: " Dynamic Response of the Hood Canal Floating Bridge", Proc. of the second speciality

conference on Dynamic Response of Structures: Experimentation, Observation, Prediction and Control, Atlanta, GA, 1981.

24. Hartz, B.J. and Georgiadis, C.: A Computer Program for the Dynamic Analysis of Continuous Floating Structures in Short Crested Waves, Technical Report, Dept. of Civil Engineering, University of Washington, Aug 1981.

25. Higgins, A.L., Seymour, R.J. and Pawka, S.S.: "A Compact Representation of Ocean Wave Directionality", Applied Ocean Research, Vol. 3, No. 3, pp. 105-112, 1981.

26. Hooft, J.P.: Advanced Dynamics of Marine Structures, Wiley, 1982.

27. Huctchison, Bruce L.: Impulse Response Techniques for Floating Bridges and Breakwaters Subject to Short-Crested Seas, paper submitted to SNAME, unpublished, Oct, 1982.

28. Jawson, M.A. and Symm, G.T.: Integral Equation Methods in Potential Theory and Elastostatics, Academic Press, London, 1977.

29. Jeffreys, E.R., Wareham, G.T., Ramsden, N.A. and Platts, M.J.: "Measuring Directional Spectra with the MLM", Proc. of the conference on Directional Wave Spectra Applications, ASCE, 1981.

30. Johnson, D.H.: "The Application of Spectral Estimation Methods to Bearing Estimation Problems", Proc. of the IEEE, Vol.70, No.9, Sep 1982.

31. Kreyszig, E.: Advanced Engineering Mathematics, Wiley, 1972

32. Lamb, H: Hydrodynamics, 6th Edition, Cambridge University Press, London, 1932.

33. Landau, L., Nelson, Ebecken, N.F.F, de Lima, E.C.P. and Ferrante, A.J. : "The Static Contribution of Higher Modes in the Dynamic Analysis of Offshore Structures", Proc. of the 3rd International Symposium on Offshore Engineering, Brazil, 1981 - Offshore Engineering, edited by Carneiro, Ferrante and Batista, Pentech Press, London, 1982.

34. Langen, I.: On Dynamic Analysis of Floating Bridges, Norwegian Institute of Technology, May 1981.

35. Langen, I. and Sigbiornsson, R.: "On Stochastic Dynamics of Floating Bridges", Engineering Structures, Vol. 2, No. 4, 1980, pp. 209-216.

36. Langen, I. and Sigbjornsson, R.: "Evaluation of Floating Bridge Behavior, Proc. of the conference on Directional Wave Spectra Applications, ASCE, 1981.

37. McGure, William and Gallagher, Richard H.: Matrix Structural Analysis, Wiley, 1979.

38. Mei, C.C.: The Applied Dynamics of Ocean Surface Waves, Wiley, New York, 1982.

39. Miller, R.W.: Rigid Body Motion of a Floating Breakwater: Seakeeping Theory Predictions and Field Measurements, Thesis, University of Washington, 1984.

40. Miksad, R.W., Powers, E.J., Kim, Y.C., Jones, F.L. Solis, R.S. and Fischer, F.J.: "Applications of Digital Time Series Techniques to Determine Non Linear Drift Forces", Proc. of the 3rd International Symposium on Offshore Engineering, Brazil, 1981 - Offshore Engineering, edited by Carneiro, Ferrante and Batista, Pentech Press, London, 1982.

41. Mukherji, B.: Dynamic Behavior of a Continuous Floating Bridge, Ph. D dissertation, University of Washington, 1972.

42. Naftzger, Robert A. and Chakrabarti, Subrata K.: "Scattering of Waves by Two-Dimensional Circular Obstacles in Finite Water Depths", Journal of Ship Reasearch, Vol. 23, No.1, Mar 1979.

43. Newman, J.N.: Marine Hydrodynamics, MIT Press, 1977.

44. Oakley, O.H. and Lozow, J.B.: "Directional Spectra Measurement by Small Arrays", Proc. Offshore Technology Conference, Vol. 1, OTC 2745, 1977.

45. Paniker, N.N: Determination of Directional Spectra of Ocean Waves from Gage Arrays, Technical Report HEL-1-18, Hydraulic Engineering Laboratory, College of Engineering, University of California, Berkely, Aug 1971.

46. Pinkster, J.A.: "Low Frequency Second Order Wave Forces on Vessels Moored at Sea", 11 th Symposium on Naval Hydrodynamics, University College, London, 1976.

47. Pinkster, J.A. and Van Oortmessen, G.: "Computation of the First and Second Order Wave Forces on Bodies Osclliating in Regular Waves", 2 nd Int. Conf. on Numerical Ship Hydrodynamics, Berkeley, 1977.

48. Pinkster, J.A.: "Mean and Low Frequency Wave Drifting Forces on Floating Structures", Ocean Engineering, Vol. 6, pp 593-615, 1979.

49. Regier, Lloyd A. and Davis, Russ E.:"Observation of the Power and Directional Spectrum of Ocean Surface Waves", Journal of Marine Research, Vol.35, No.3, 1977.

50. Regier, Lloyd A. and Davis, Russ E.: "Methods for Estimating Wave Spectra from Multi-Element Arrays", Journal of Marine Research, Vol.35, No.3, 1977.

51. Salvesen, N., Tuck, E.O. and Faltinsen, O.: "Ship Motions and Sea Loads", Trans. SNAME, 1970.

52. Sarpkaya,Turgut and Isaacson, Michael : Mechanics of Wave Forces on Offshore Structures, Van Nostrand Reinhold Co., 1981.

53. Sayer, P. and Ursell, F. : "Integral Equation Methods for Calculating the Virtual Mass in Water of Finite Depth", Second International Conference on Numerical Ship Hydrodynamics, Sep 1977.

54. Schmitke, Rodney T.: "Ship Sway, Roll and Yaw Motions in Oblique Seas", SNAME Proceedings, 1978.

55. Sigbjornsson, R. : "Stochastic Theory of Wave Loading Processes", Engineering Structures, Vol. 1, 1979, pp.58-64.

56. Standing, R.G. : Use of Potential Flow Theory in Evaluating Wave Forces on Offshore Structures, report submitted to Department of Energy, Offshore Technology Board.

57. Standing, R.G., Dacunha, N.M.C. and Matten, R.B.: Mean Wave Drift Forces: Theory and Experiment, National Maritime Institute, Feltham, England, 1981.

58. Standing, R.G., Dacunha, N.M.C. and Matten, R.B.: Slowly Varying Second Order Forces: Theory and Experiment, National Maritime Institute, Feltham, England, 1981.

59. Taylor, R. Eatock: "Generalized Hydrodynamic Forces on Vibrating Structure by Wave Diffraction Techniques", Proc. of the Int. Conference on Offshore Structures

Engineering, Brazil, 1977 - Offshore Structures Engineering, edited by Carneiro, Ferrante and Brebbia, Pentech Press, London, 1979.

60. Thomson, D.J. : "Spectral Estimation and Harmonic Analysis", Proc. of the IEEE, Vol.70, N0.9, Sep 1982

61. Triantafyllou, M.S., Bodson, M. and Athans, M.: "Real Time Estimation of Ship Motions using Kalman Filtering Techniques", IEEE Journal of Oceanic Engineering, Vol. OE-8, No.1, Jan 1983.

62. Vugts, J.H., Hines, I.M., Nataraja, R. and Schumm, W.: "Modal Superposition Vs Direct Solution Techniques in the Dynamic Analysis of Off-Shore Structures", Proc. of the Second Annual Conference on the Behavior of Off-Shore Structures, London, England, 1979.

63. Vugts, J.H.: The Hydrodynamic Forces and Ship Motions in Waves, Ph.D thesis, Technische Hogeschool Delft, Uitgeverij Waltman, Delft, 1970.

64. Wehausen, J.V. and Laitone, E.V.: "Surface Waves", Encyclopedia of Physics, Springer-Verlag, Berlin, 1960.

65. Willems, Nicholas and Lucas, William M.: Matrix Analysis for Structural Engineers, Prentice Hall, 1968.

66. Zienkiewicz, O.C.: The Finite Element Method, McGraw-Hill, 1977.

APPENDIX A

We need to minimize

$$S_\eta(\theta_d, w) = \mathbf{A}_d^{*T}\, \mathbf{Q}(w)\, \mathbf{A}_d$$

subject to the constarint $|\mathbf{A}_d^{*T}\, \mathbf{r}(w,\theta_d)| = 1$

This is a typical Lagrange multiplier problem. Therefore, the above problem simplifies to minimizing

$$L = \mathbf{A}_d^{*T}\, \mathbf{Q}(w)\, \mathbf{A}_d + (\mathbf{A}_d^{*T}\, \mathbf{r}(w,\theta_d) - z)$$

where z is a complex number with unit magnitude.

Setting, $\partial L/\partial \mathbf{A}_d^* = \emptyset$ gives

$$\mathbf{Q}(w)\, \mathbf{A}_d + \lambda \mathbf{r}(w,\theta_d) = \emptyset \qquad \text{(i)}$$

$\partial L/\partial \lambda = \emptyset$ gives

$$\mathbf{A}_d^{*T}\, \mathbf{r}(w,\theta_d) - z = \emptyset \qquad \text{(ii)}$$

Substituting for $\mathbf{A}_d = -\lambda \mathbf{Q}^{-1}\, \mathbf{r}$ from (i) in (ii),

$$\lambda = -\frac{z^*}{\mathbf{r}^T\, [\mathbf{Q}^{-1}]^T\, \mathbf{r}^*}$$

Substituting for λ in (i) gives $\mathbf{A}_d$,

$$\mathbf{A}_d = \frac{z^*\, \mathbf{Q}^{-1}\, \mathbf{r}}{\mathbf{r}^T\, [\mathbf{Q}^{-1}]^T\, \mathbf{r}^*}$$

Substituting for $\mathbf{A}_d$ in the expression for $S_\eta(\theta_d, w)$ we get

$$S_\eta(\theta_d, w) = 1 \,/\, [\mathbf{r}^{*T}(w,\theta_d)\, \mathbf{Q}^{-1}(w)\, \mathbf{r}(w,\theta_d)]$$

APPENDIX B

The cross-correlation matrix of force vectors for elements i and j is given by

$$R_{f\ i,j}(\tau) = E[f_i(t) f_j(t+\tau)^{*\ T}]$$

$$= \int_{\theta} \left[\int_{l_1} \int_{l_2} \mathbf{N}_i^T \mathbf{f}(\theta,w) \mathbf{f}(\theta,w)^{*\ T} \mathbf{N}_j \exp\{i[k(z_i - z_j)\sin\theta\} \right.$$

$$\left. dl_1 dl_2 \right] \exp(iw\tau)\ S_{\eta}(\theta,w)\ d\theta dw$$

To obtain the spectral matrix, the above expression has to be fourier transformed. It can be seen that the cross-correlation matrix is in the form

$$\int P(w)\ \exp(iw\tau)\ d\omega$$

which can be easily recognized as a backward fourier transform. Therefore if we forward fourier transform the cross correlation matrix, the result should be equal to $P(w) = S_{fi,j}$. i.e. the hydrodynamic force spectral matrix is given by,

$$\mathbf{S_{fi,j}(w)} = \int_{\theta} \left[\int_{l_1} \int_{l_2} \mathbf{N}_i^T \mathbf{f}(\theta,w) \mathbf{f}(\theta,w)^{*\ T} \mathbf{N}_j \exp\{i[k(z_i - z_j)\sin\theta\} \right.$$

$$\left. dl_1 dl_2 \right] S_{\eta}(\theta,w)\ d\theta$$

APPENDIX C

$$p = - \rho g y - \rho \partial \phi / \partial t - (1/2)\ \rho (\nabla \phi)^2$$

Substituting $\phi = \varepsilon \phi_1 + \varepsilon^2 \phi_2$

$$p = p_\emptyset + \varepsilon p_1 + \varepsilon^2 p_2$$

$$y = y_\emptyset + \varepsilon y_1$$

and considering second order terms,

$p_2 = - \rho \partial \phi_{2,\emptyset} / \partial t$ - [O(2) terms of $- \rho \partial \phi_1 / \partial t$] $-(1/2) \rho (\nabla \phi 1,\emptyset)^2$

where the additional $\emptyset$ in the subscript indicates that the potential has been computed at the mean position of the point under consideration. To consider the O(2) portions of the second term of the above expression we use Taylor expansion to express ϕ_1 about its mean position as,

$$\phi_1 = \phi_{1,\emptyset} + \nabla \phi_{1,\emptyset} \cdot \mathbf{s}_1 + \text{higher order terms}$$

Then, the second term $= - \rho (\partial / \partial t)(\mathbf{s}_1 \cdot \nabla \phi_{1,\emptyset})$

$$= - (\mathbf{s}_1 \cdot \nabla \partial \phi_{1,\emptyset} / \partial t)$$

With the understanding that all potentials used are computed at the mean position of the structure, we can drop the zero in the potential subscript which gives,

$$p_2 = \text{second order pressure} = - (1/2) \rho\ (\nabla \phi_1)^2 - \rho \partial \phi_2 / \partial t - (\mathbf{s}_1 \cdot \nabla \partial \phi_1 / \partial t)$$

$s_1 = (x_1, y_1)$ is the first order displacement of the center of gravity of the section.

APPENDIX D

Multivariate Spectral Analysis of Time Series

Suppose we observe n different events (or time series) X_1, X_2,....X_n at a given time t. In general, the observations can be complex. It is possible to arrange these n observations in a vector $\mathbf{X}(t)$;

$$\mathbf{X}(t) = [X_1(t) \quad X_2(t) \; .. \; X_n(t)]^T$$

Assume that the mean of all the events are zero for convenience. The correlation function at lag k is then a n x n matrix given by

$$\mathbf{C}(k) = E[\mathbf{X}(t)\ \mathbf{X}^{*T}(t+k)]$$

$$= E\begin{bmatrix} X_1(t)X_1^*(t+k) & X_1(t)X_2^*(t+k) & \cdots & X_1(t)X_n^*(t+k) \\ X_2(t)X_1^*(t+k) & X_2(t)X_2^*(t+k) & \cdots & X_2(t)X_n^*(t+k) \\ \cdots & \cdots & \cdots & \cdots \\ X_n(t)X_1^*(t+k) & X_n(t)X_2^*(t+k) & \cdots & X_n(t)X_n^*(t+k) \end{bmatrix}$$

$$= \begin{bmatrix} C_{11}(k) & C_{12}(k) & \cdots & C_{1n}(k) \\ C_{21}(k) & C_{22}(k) & \cdots & C_{2n}(k) \\ \cdots & \cdots & \cdots & \cdots \\ C_{n1}(k) & C_{n2}(k) & \cdots & C_{nn}(k) \end{bmatrix}$$

For a stationary event (or process, or time series) the correlation depends on on the time lag only. The diagonal elements are the auto-correlation functions of each event and the off-diagonal terms are the cross-correlation functions for each

pair of events. It is easy to see that **C** is hermitian (i.e $C_{ij} = C_{ji}^{*}$).

The spectral density matrix **S**(w) is given by fourier transforming **C**,

$$\mathbf{S}(w) = \int_{-\infty}^{\infty} \mathbf{C}(\tau) \exp(-iw\tau)\, d\tau$$

$$= \begin{vmatrix} S_{11}(w) & S_{12}(w) & \cdots & S_{1n}(w) \\ S_{12}(w) & S_{12}(w) & \cdots & S_{2n}(w) \\ \cdots & \cdots & \cdots & \cdots \\ S_{n1}(w) & S_{n2}(w) & \cdots & S_{nn}(w) \end{vmatrix}$$

Again, the diagonal terms are called the Auto-Spectral Density of each event and the off-diagonal terms give the the cross-spectral density for each pair of events. If all the events are assumed to be Gaussian, knowing the spectral matrix above means that all the statistics of the joint events are known and statistically similar such events can be reconstructed. It is easy to see that interpretation of the cross spectral density is difficult in its dimensional form, as for example the two events considered can have different units or scale effects etc. Coherence and Phase is therefore defined to avert this difficulty as follows (for two events i and j)

$$\text{Coherence } Ch_{ij}(w) = \frac{\text{Real}[S_{ij}(w)]^2 + \text{Imag}[S_{ij}(w)]^2}{S_{ii}(w)\ S_{jj}(w)}$$

Phase $\theta_{ij}(w) = - \text{Tan}^{-1} [\text{Real}[S_{ij}(w)] / \text{Imag}[S_{ij}(w)]$

Ch(w) always takes a value between Ø and 1. This is a measurement of how linearly related the two processes are in the frequency domain.

Example 1:

The events $X_1(t)$, $X_2(t),\ldots,X_n(t)$ can be the the time series at directional wave gages at n locations. **S**(w) then becomes the Cross Power Spectral Density Matrix (CPSD) = **Q**.

Example 2:

Consider the construction of the hydrodynamic force sepctral matrix. The events $X_1(t)$, $X_2(t),\ldots,X_n(t)$ are now the Hydrodynamic force time series for all degrees of freedom. If there are N number of nodes and M degrees of freedom at each node (e.g M = 2 for heave), then n = (N)(M).

Table 1. Normalized Hydrodynamic Coefficients for the West Point Floating Breakwater Pontoon
B = 16 ft T = 3.5 ft

Freq(hz)	SIGMA	a(1,1)	c(1,1)	a(2,2)	c(2,2)	a(3,3)	c(3,3)	a(1,3)	c(1,3)
.100	.3131	.708781E 0	.130371E -1	.208731E 1	.936403E 0	.697519E -1	.346411E -3	-.355947E -1	-.201336E -2
.200	.6263	.826425E 0	.200503E 0	.178477E 1	.103188E 1	.682646E -1	.339241E -2	-.428389E -1	-.242548E -1
.300	.9394	.459601E 0	.601934E 0	.159840E 1	.782570E 0	.623444E -1	.437518E -2	.877520E -2	-.468611E -1
.400	1.2526	.146114E 0	.639106E 0	.175619E 1	.403503E 0	.623572E -1	.113308E -2	.250885E -1	-.230865E -1
.500	1.5657	.439499E -1	.540817E 0	.205640E 1	.180231E 0	.637520E -1	.154988E -4	.177248E -1	-.121029E -2

sigma = non-dimensional frequency
$= w\sqrt{B/2g}$

Table 2. Normalized Hydrodynamic Force Coefficients for the West Point Floating Breakwater Pontoon
B = 16 ft T = 3.5 ft

Freq .1000 Hz (.6283 r/s)
Non dimensional freq .313148
Wave number .01745
Wave length 360.129

Theta(deg)	Sway	Phase	Heave	Phase	Roll	Phase
.000	.136958E 1	-.906543E 2	.872028E 0	.758603E 1	.707665E 0	.891924E 2
15.000	.134865E 1	-.912952E 2	.924570E 0	.755993E 1	.706462E 0	.881896E 2
30.000	.120112E 1	-.910372E 2	.913069E 0	.810215E 1	.625371E 0	.885742E 2
45.000	.967859E 0	-.916582E 2	.884864E 0	.408666E 1	.499771E 0	.877525E 2
60.000	.689528E 0	-.908316E 2	.909384E 0	.792689E 1	.355450E 0	.889132E 2

Freq .2000 Hz (1.2566 r/s)
Non dimensional freq .626296
Wave number .04972
Wave length 126.383

Theta(deg)	Sway	Phase	Heave	Phase	Roll	Phase
.000	.126846E 1	-.941522E 2	.611189E 0	.276412E 2	.541031E 0	.848312E 2
15.000	.914698E 0	-.980250E 2	.689026E 0	.593448E 1	.361074E 0	.901601E 2
30.000	.116202E 1	-.101730E 3	.617007E 0	.318483E 2	.498428E 0	.756046E 2
45.000	.963895E 0	-.103747E 3	.709636E 0	.310065E 2	.421742E 0	.721164E 2
60.000	.546365E 0	-.900000E 2	.612943E 0	-.652174E -6	.214451E 0	.900000E 2

Table 3. Normalized Hydrodynamic Force Coefficients for the West Point Floating Breakwater Pontoon
B = 16 ft T = 3.5 ft

Freq .3000 Hz (1.8850 r/s)
Non dimensional freq .939444
Wave number .11032
Wave length 56.958

Theta(deg)	Sway	Phase	Heave	Phase	Roll	Phase
.000	.901019E 0	-.979123E 2	.426458E 0	.648991E 2	.249462E 0	.815255E 2
15.000	.742758E 0	-.944210E 2	.215006E 0	.989735E 1	.210042E 0	.890096E 2
30.000	.633495E 0	-.110835E 3	.372245E 0	.274332E 2	.179182E 0	.804590E 2
45.000	.491751E 0	-.998851E 2	.356585E 0	.986959E 1	.139967E 0	.839472E 2
60.000	.439687E 0	-.900000E 2	.287895E 0	-.173364E -5	.113896E 0	.900000E 2

Freq .4000 Hz (2.5133 r/s)
Non dimensional freq 1.252592
Wave number .19612
Wave length 32.037

Theta(deg)	Sway	Phase	Heave	Phase	Roll	Phase
.000	.475118E 0	-.780439E 2	.316781E 0	.958910E 2	.676917E -1	.988802E 2
15.000	.463747E 0	-.899026E 2	.111988E 0	.178907E 3	.567853E -1	.899989E 2
30.000	.451157E 0	-.950078E 2	.818037E -1	.963789E 2	.570215E -1	.934596E 2
45.000	.373289E 0	-.950079E 2	.728150E -1	.164628E 2	.537220E -1	.926204E 2
60.000	.335439E 0	-.900000E 2	.868698E -1	-.920332E -5	.386827E -1	.900000E 2

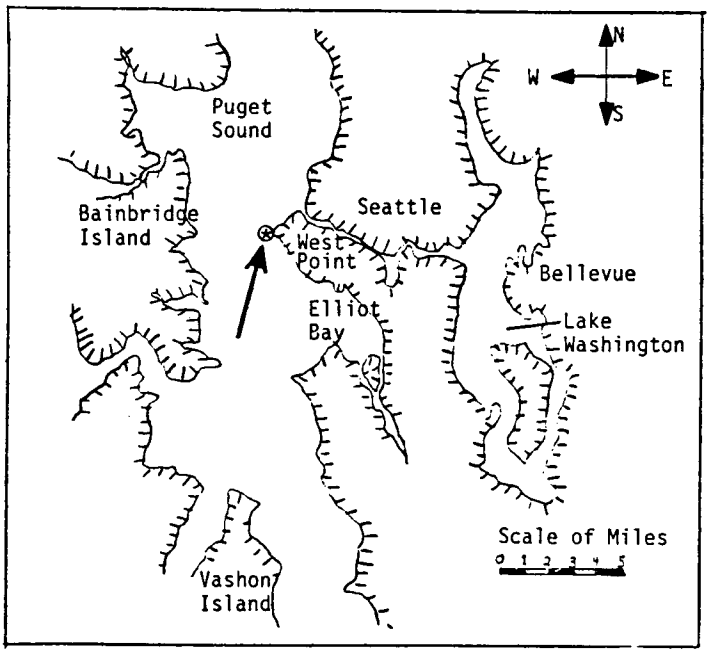

Figure 1. West Point Prototype Floating Breakwater Test Site Location

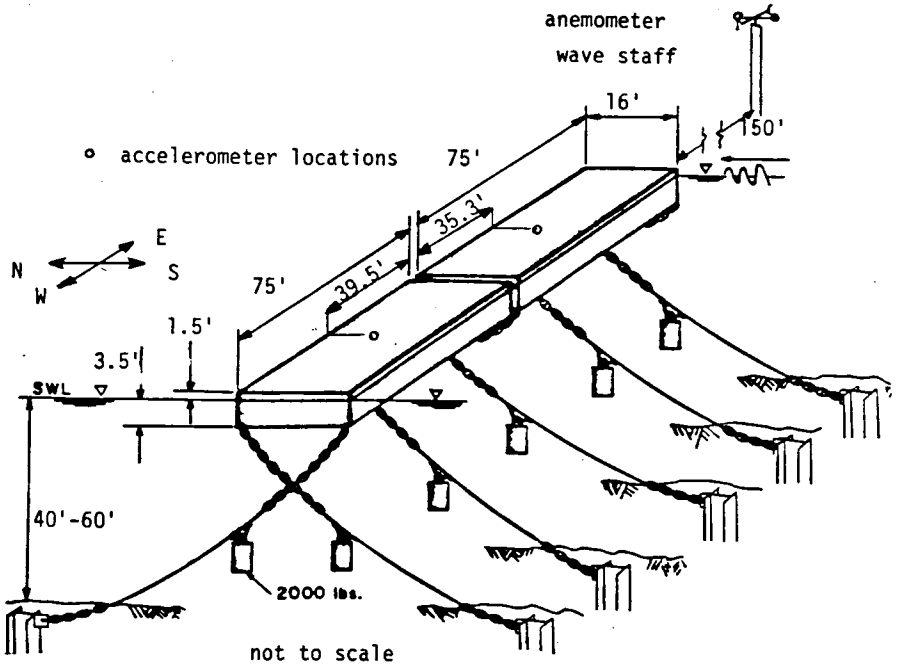

Figure 2. Pontoon Dimensions and Clump Weights

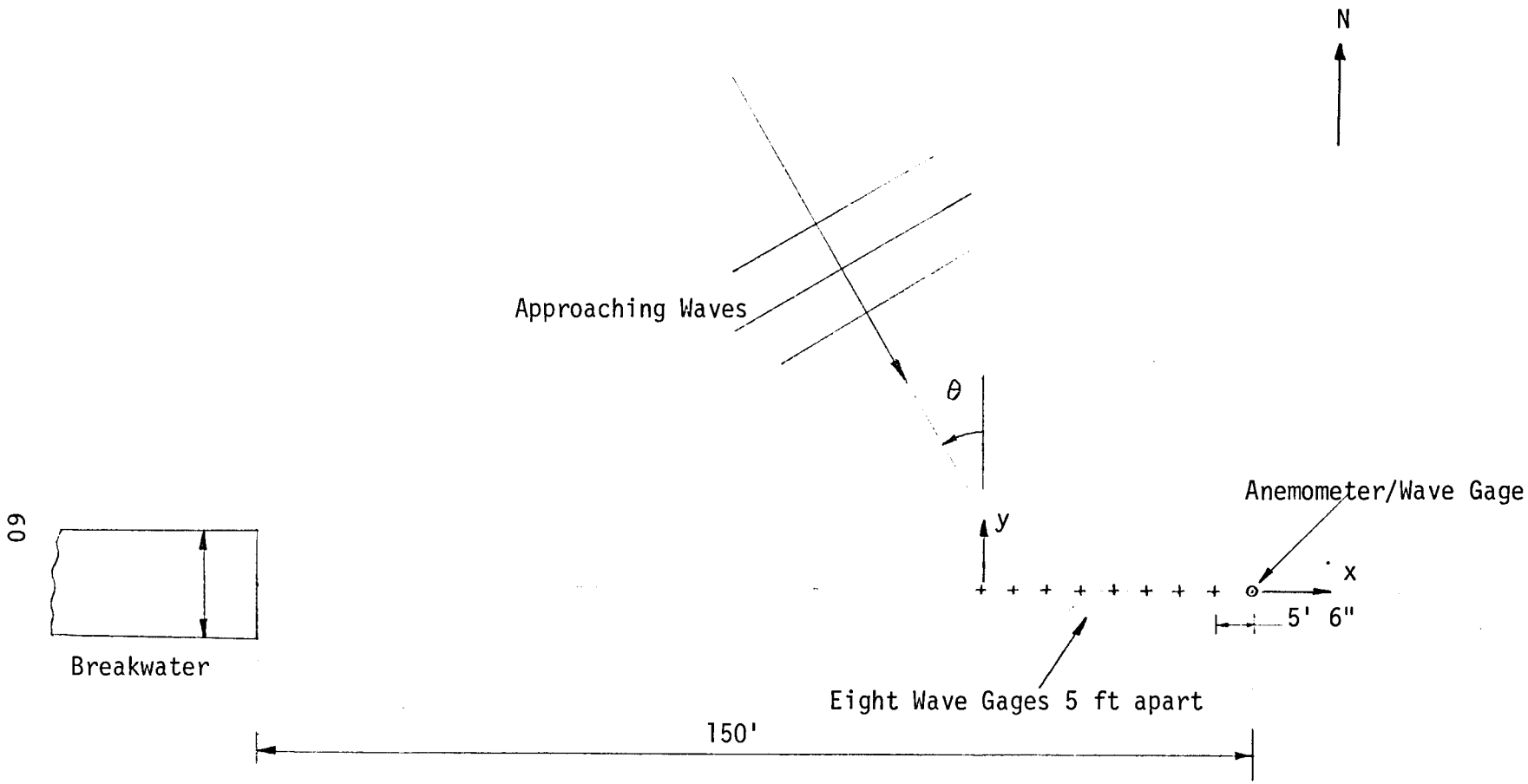

Figure 3. Gage Layout for Directional Wave Measurements

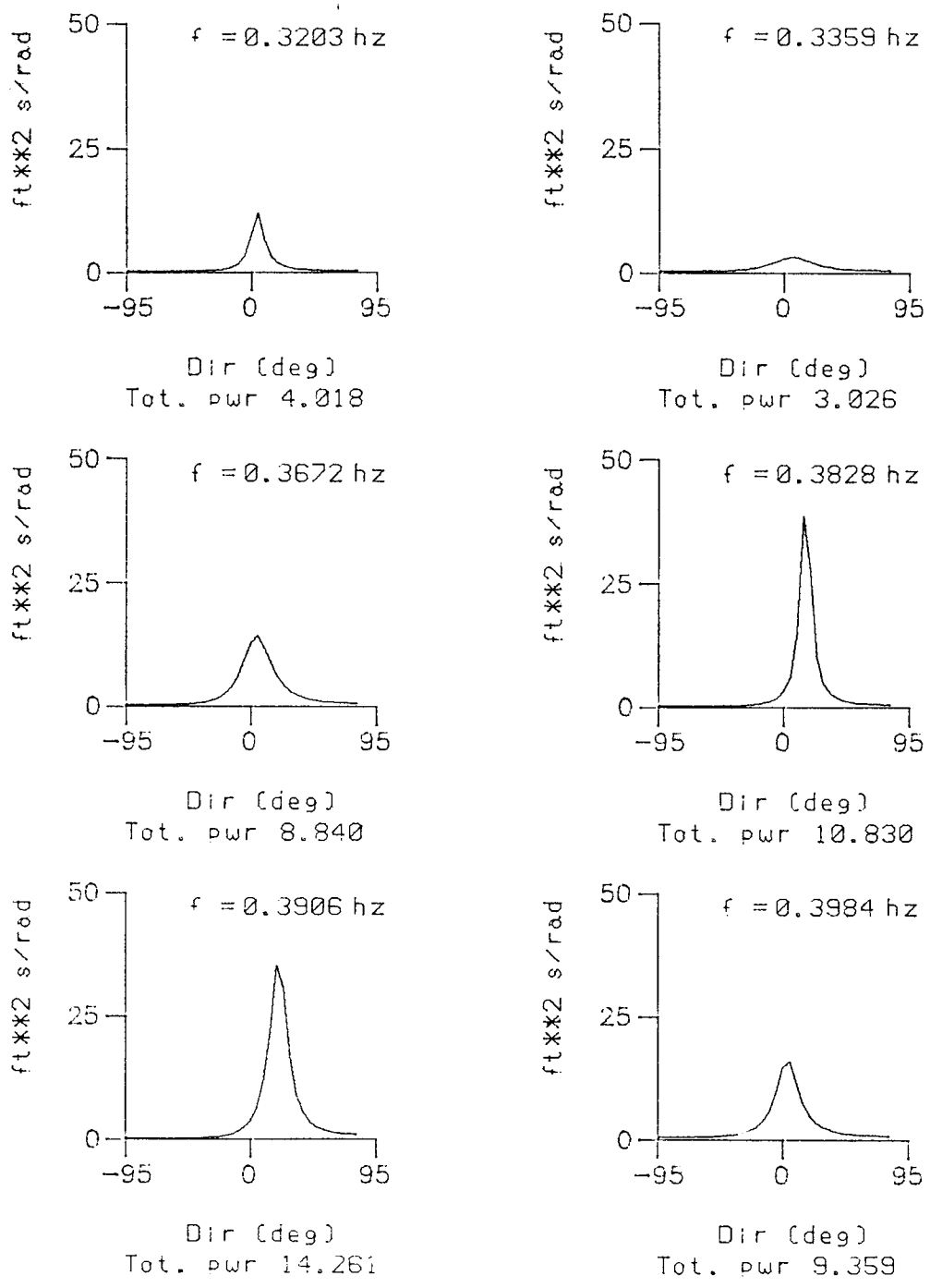

Figure 4. Directional Wave Spectra at the West Point Floating Breakwater Site - 10/21/83 00:40 hrs
BW86R6

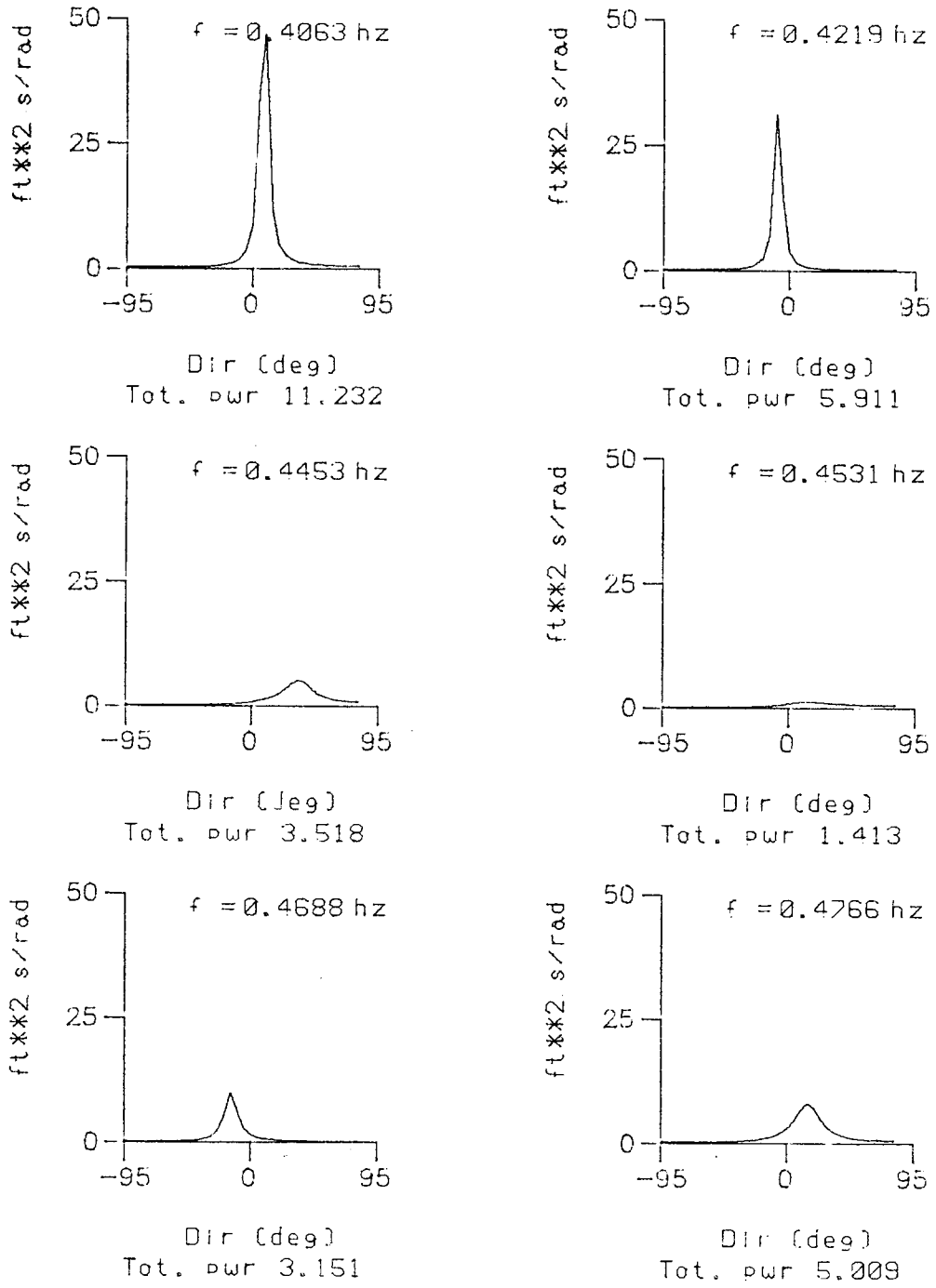

Figure 5. Directional Wave Spectra at the West Point Floating Breakwater Site - 10/23/83 00:40 hrs
BW86R6

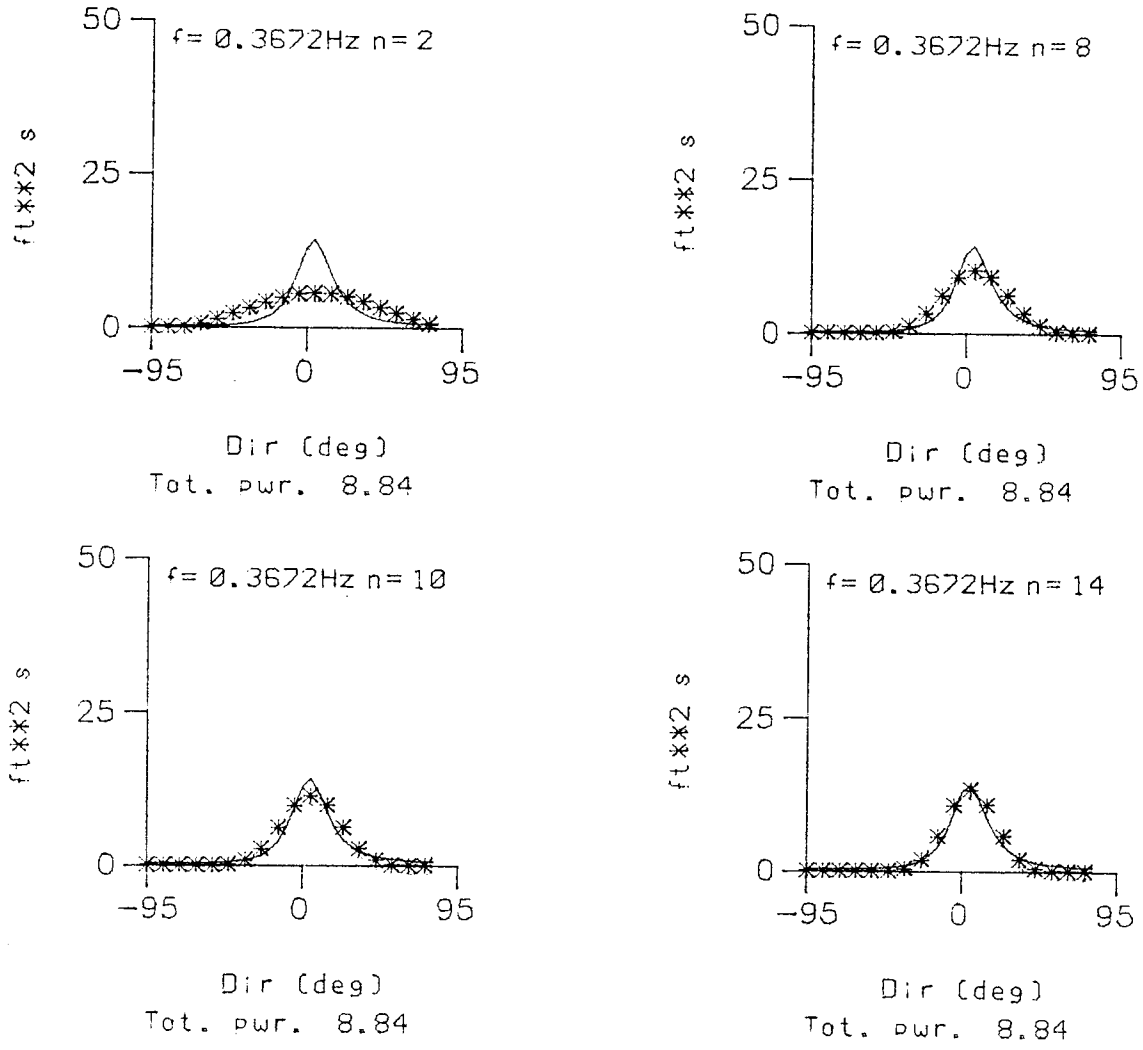

Figure 6. Comparison of C $\cos^{n}(\theta-\bar{\theta})$ with Measured Directional Wave Spectrum

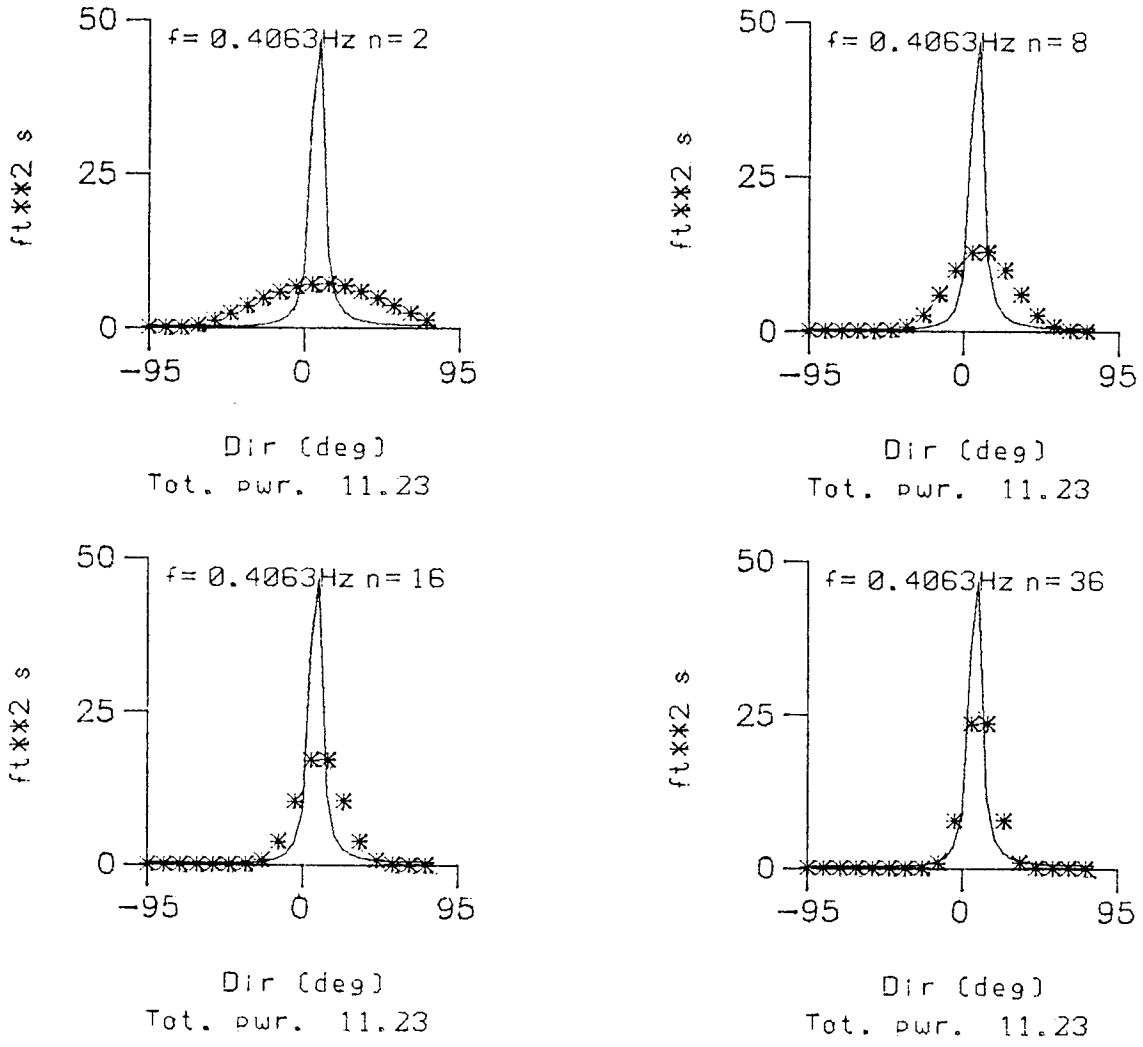

Figure 7. Comparison of C $\cos^n(\theta-\bar{\theta})$ with Measured Directional Wave Spectrum

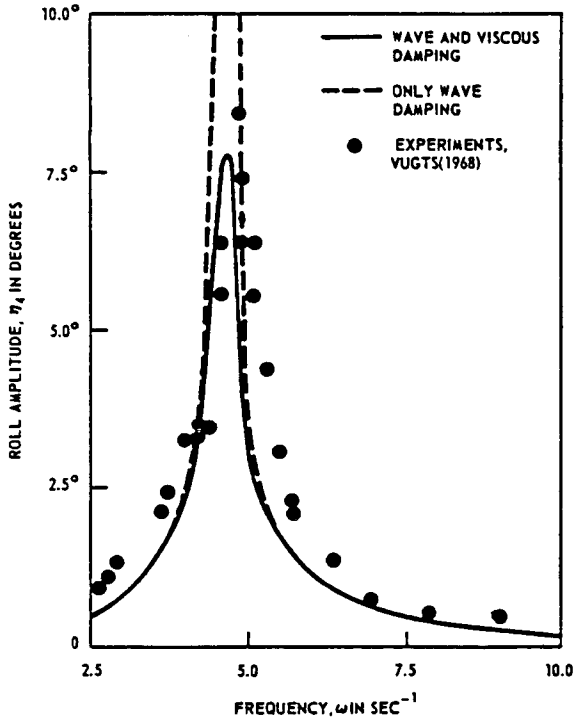

Figure 8. Theoretical and Experimental Roll Motion Amplitude for a Rectangular Cylinder in Beam Waves [Vugts]

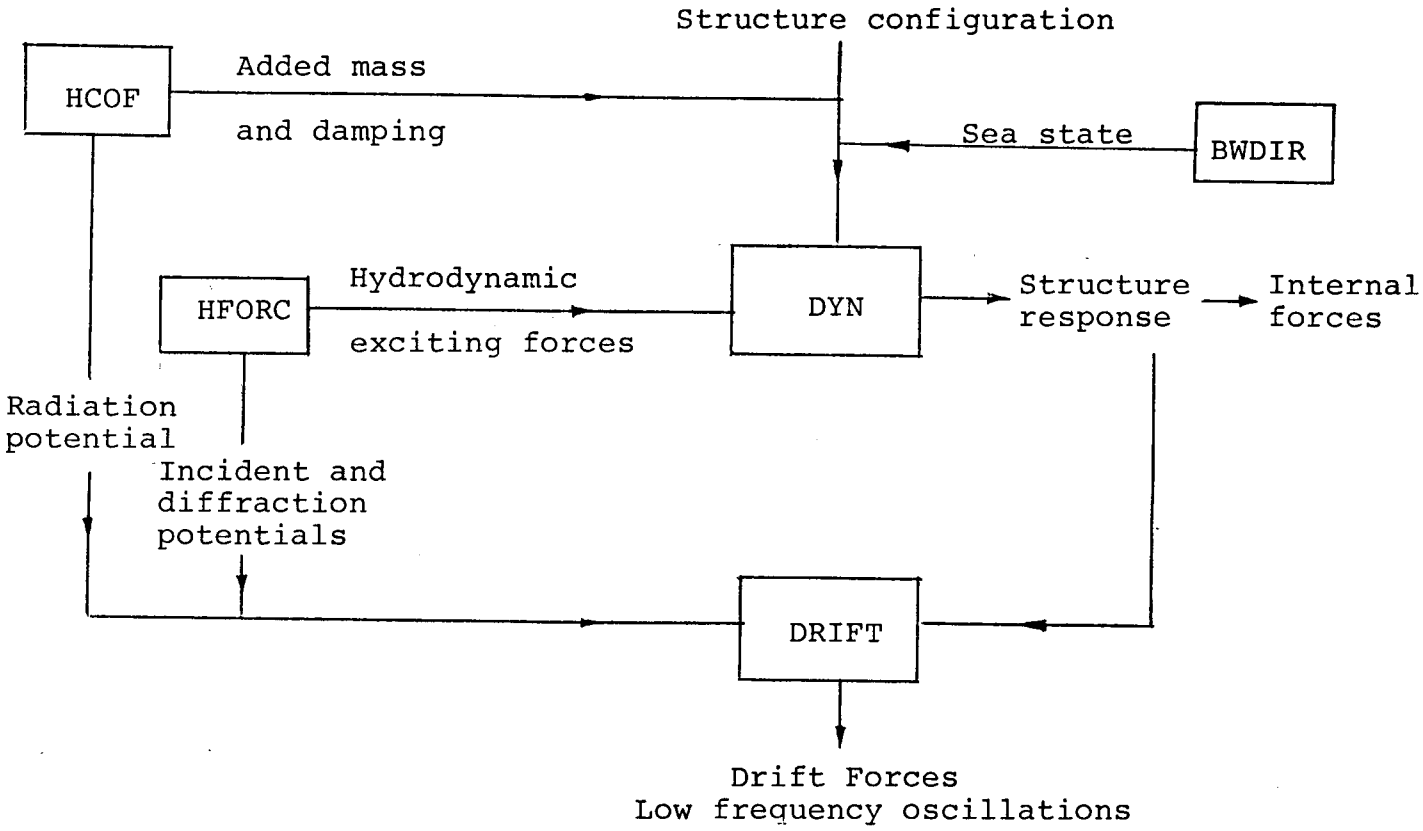

Figure 9. Program Layout for Dynamic Analysis of the Floating Breakwater

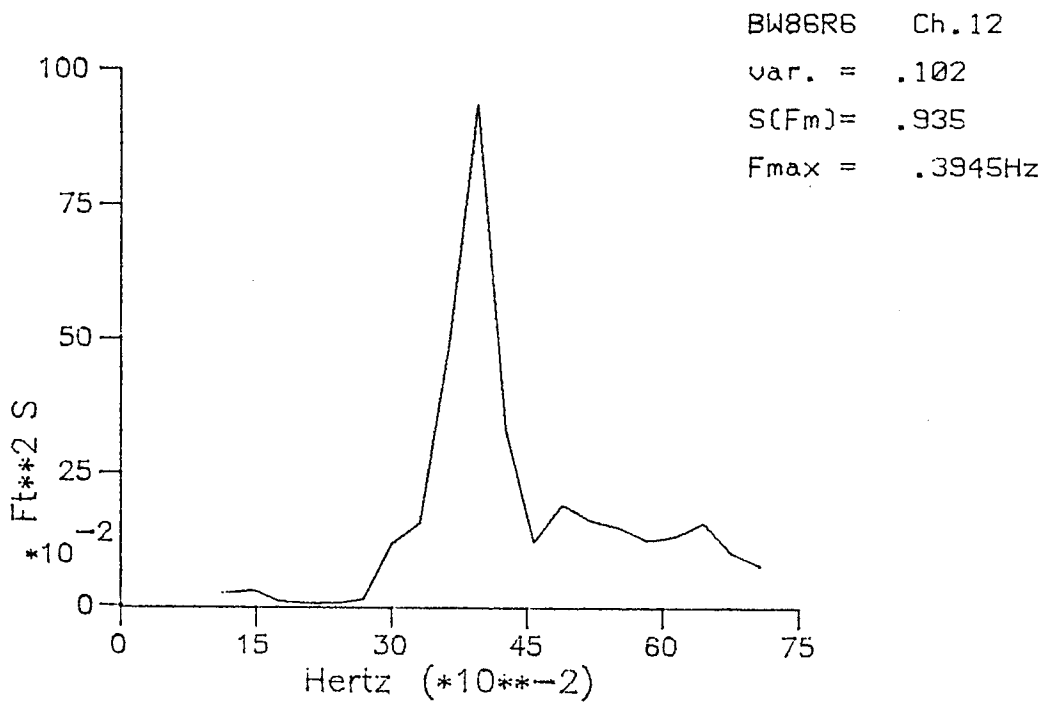

Figure 10. Example Point Wave Spectrum at West Point Breakwater Site

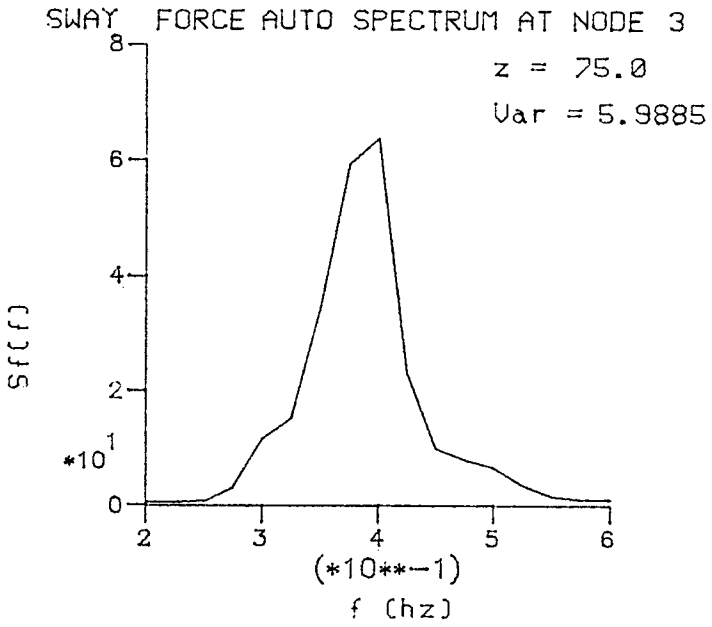

Figure 11. Hydrodynamic Sway Force Auto Spectrum at Mid-point

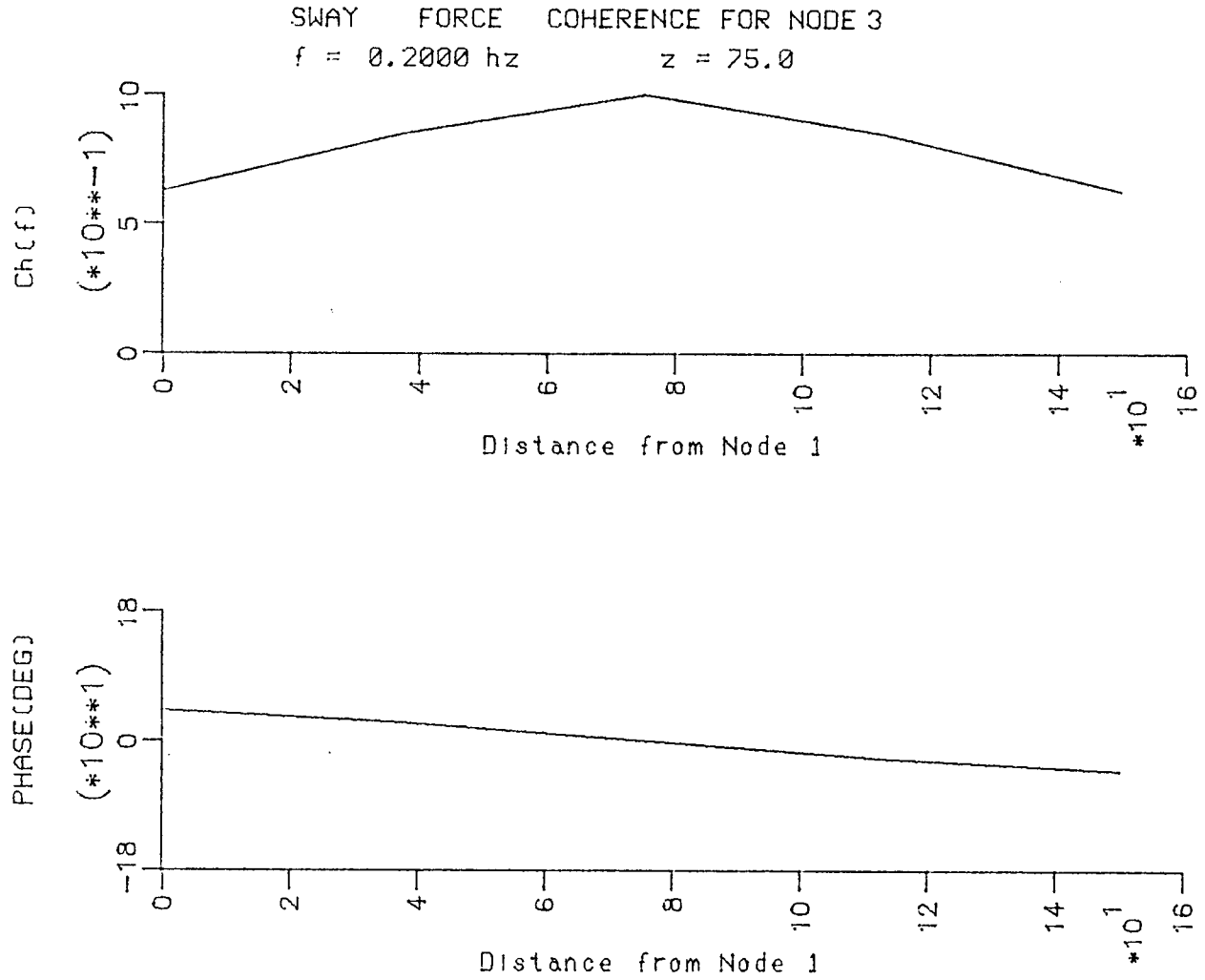

Figure 12. Coherence and Phase between Sway Force at Mid-point and Sway Force along the Structure at 0.2 hz

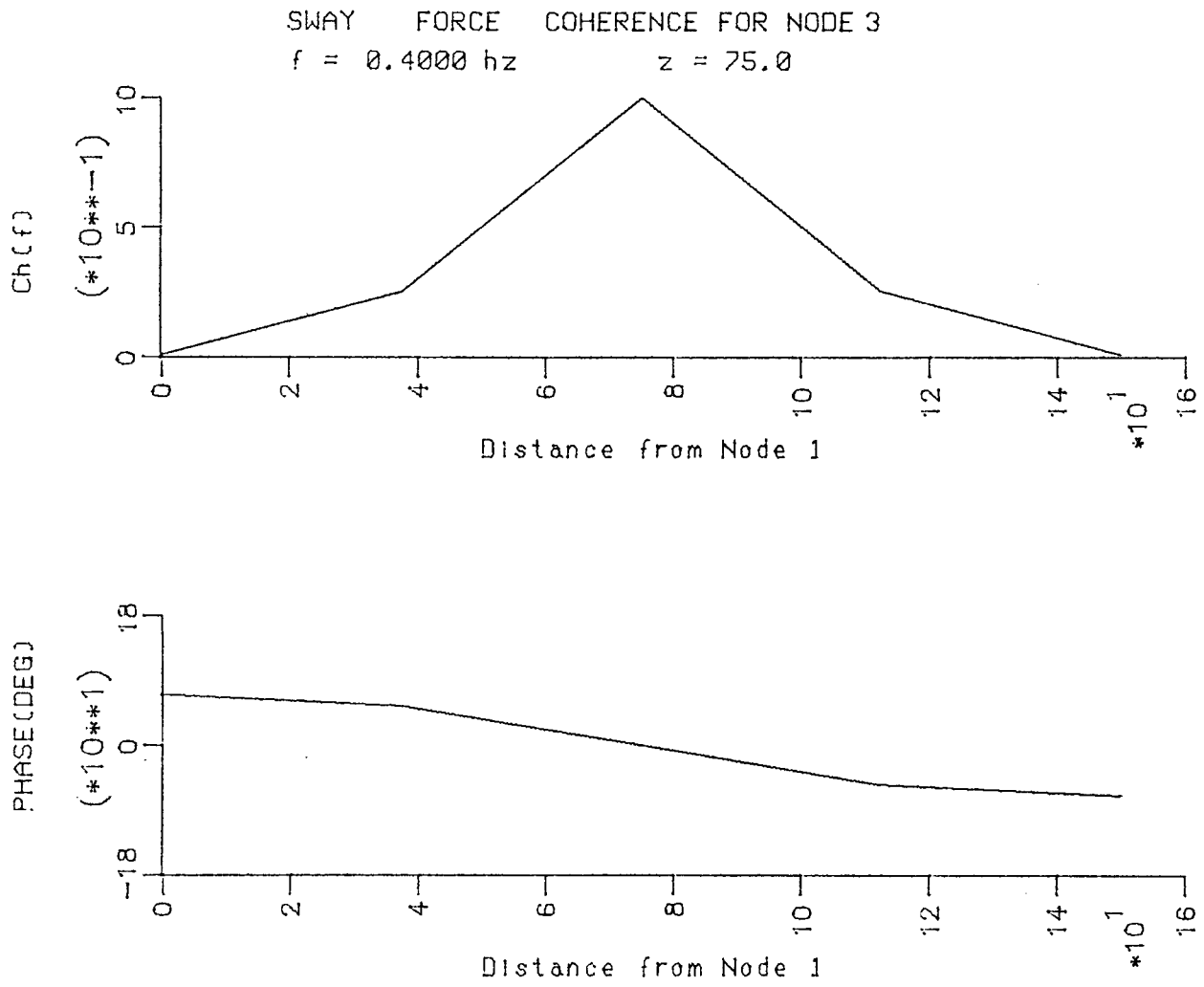

Figure 13. Coherence and Phase between Sway Force at Mid-point and Sway Force along the Structure at 0.4 hz

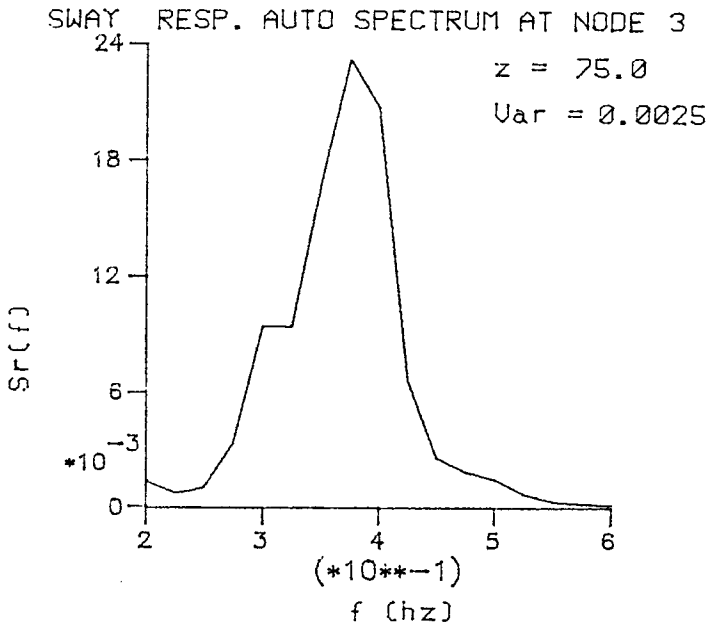

Figure 14. Sway Response Auto Spectrum at Mid-point in Ft^2S

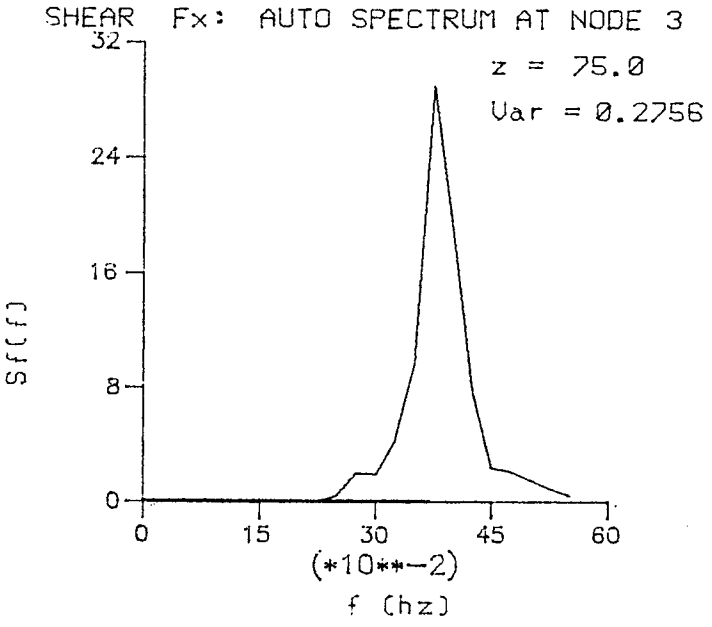

Figure 15. Horizontal Structural Shear Force Auto Spectrum at Mid-point in Kip^2S

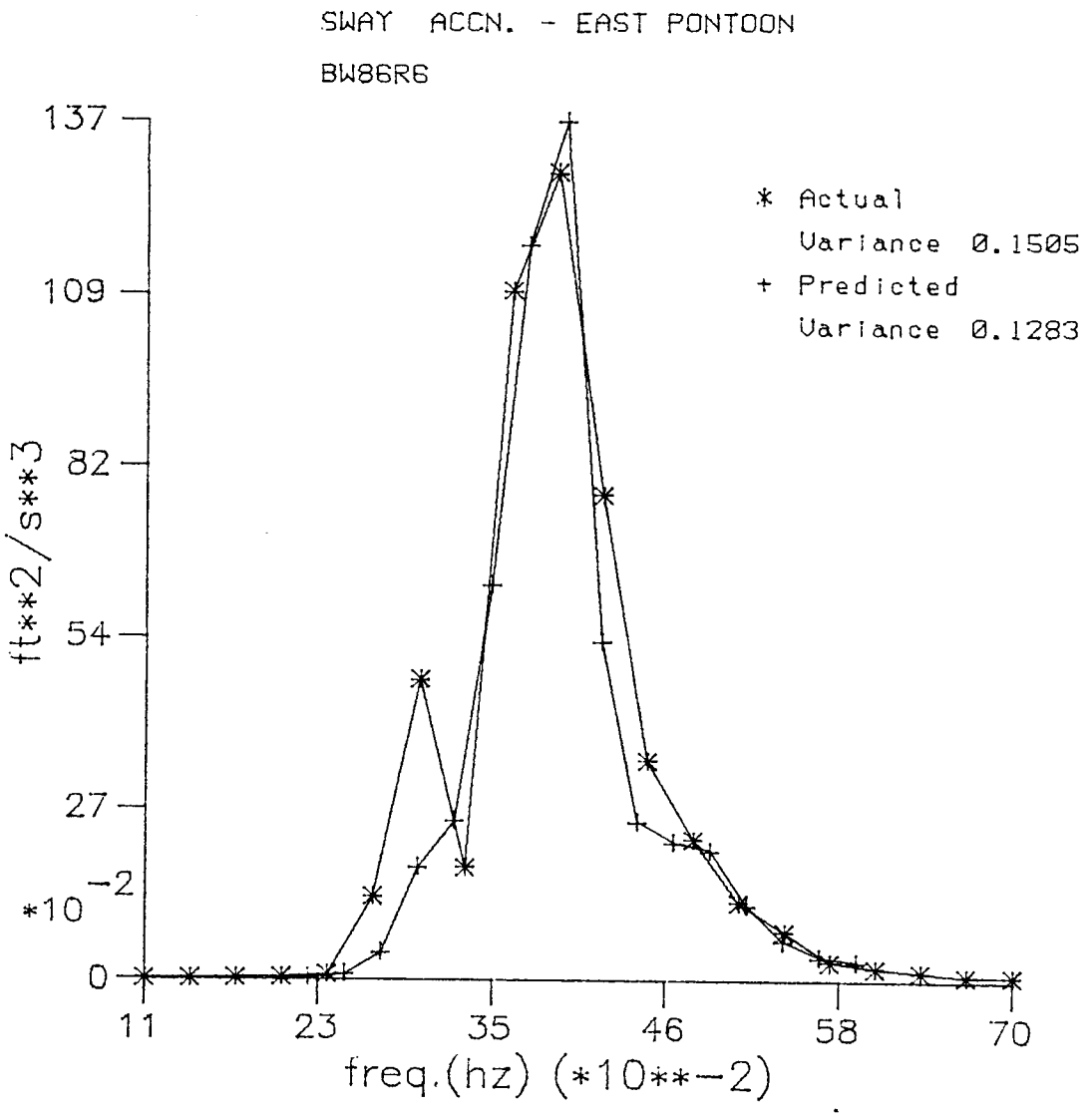

Figure 16. Predicted and Measured Sway Accelleration Auto Spectrum - East Pontoon

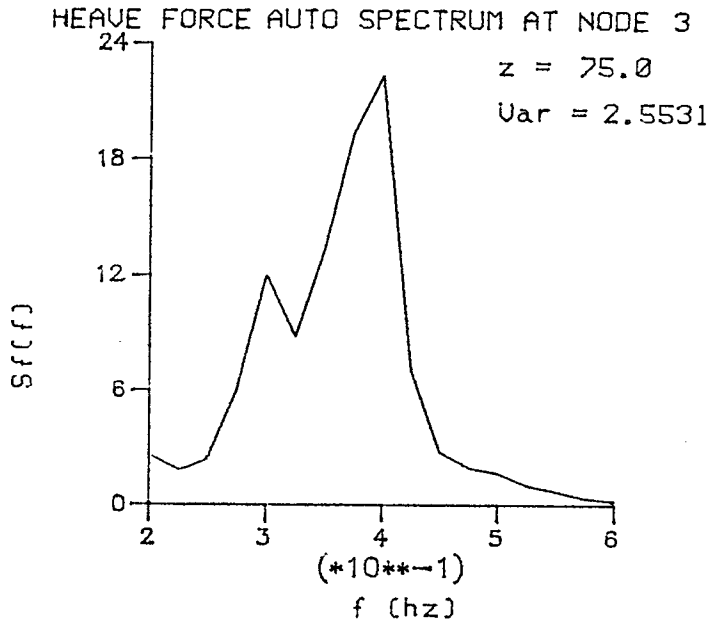

Figure 17. Heave Force Autospectrum at Mid Point in KIP^2 S

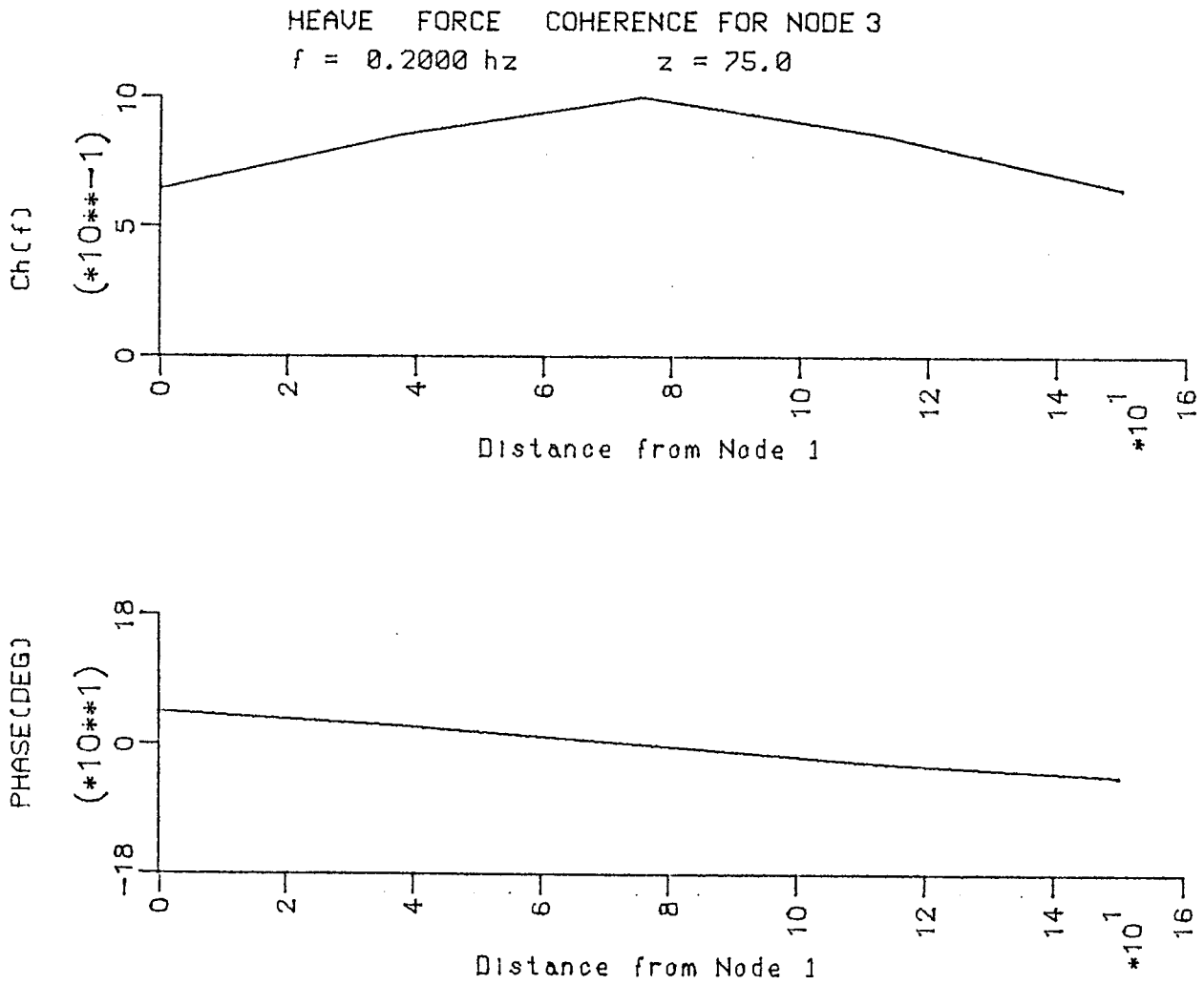

Figure 18. Coherence and phase between heave force at mid-point and heave force along the structure at .2 hz

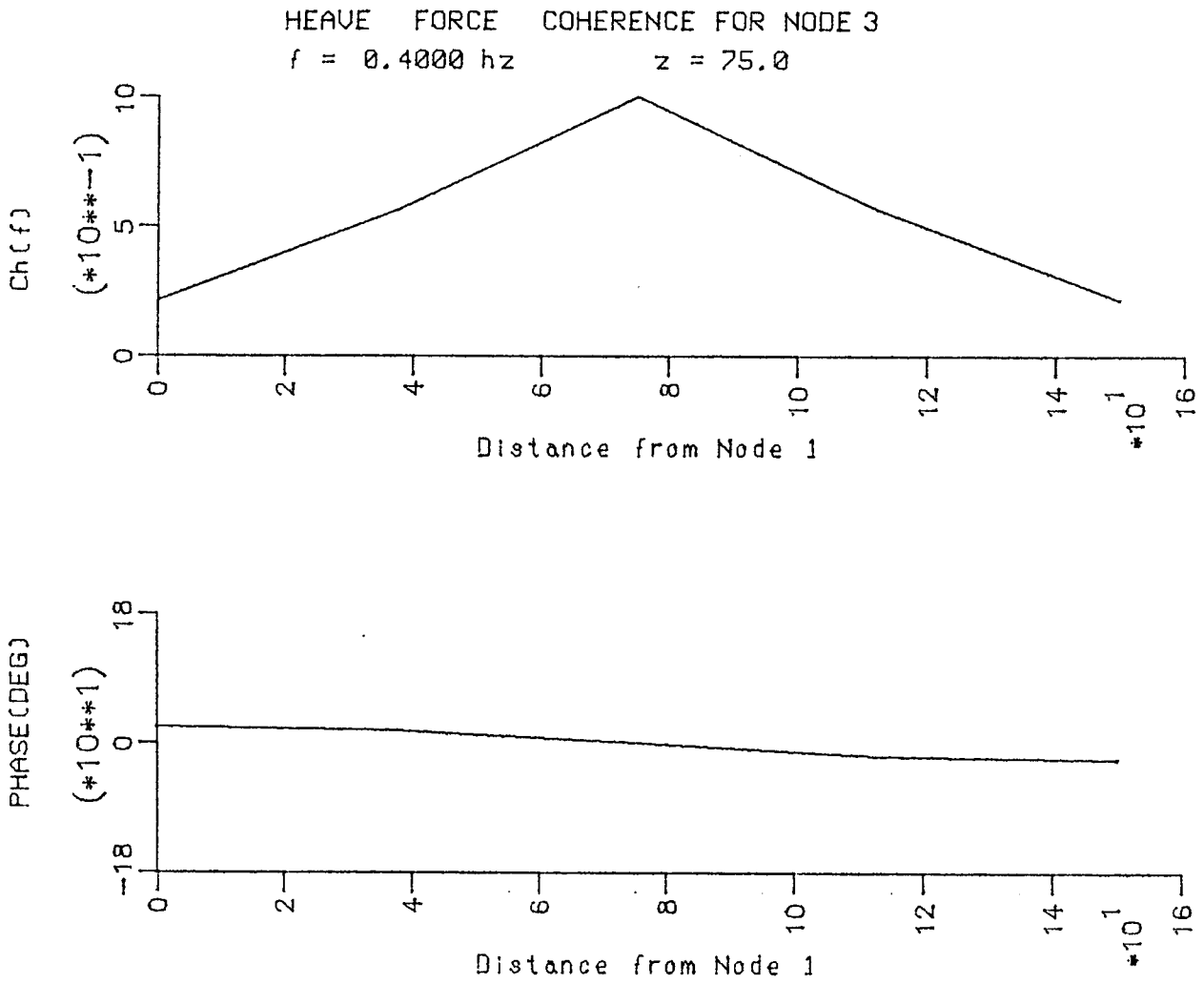

Figure 19. Coherence and phase between heave force at mid-point and heave force along the structure at .4 hz

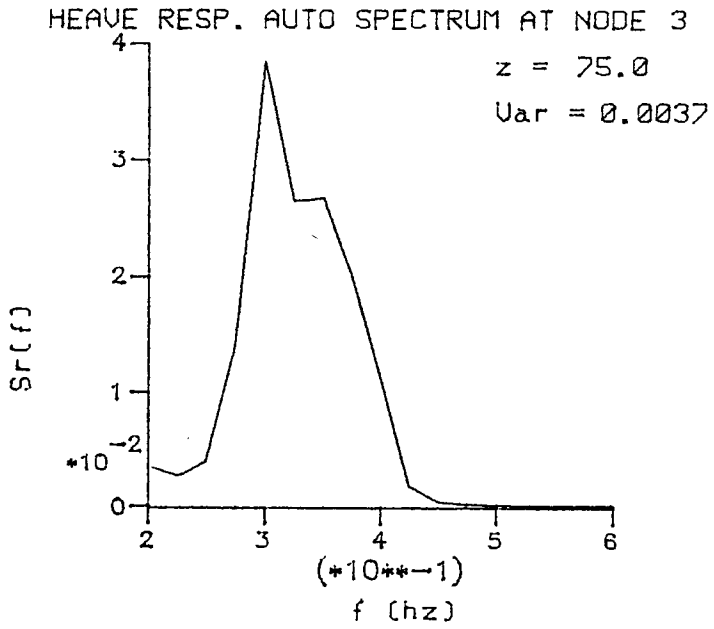

Figure 20. Heave Response Auto Spectrum at Mid-Point in FT^2 S

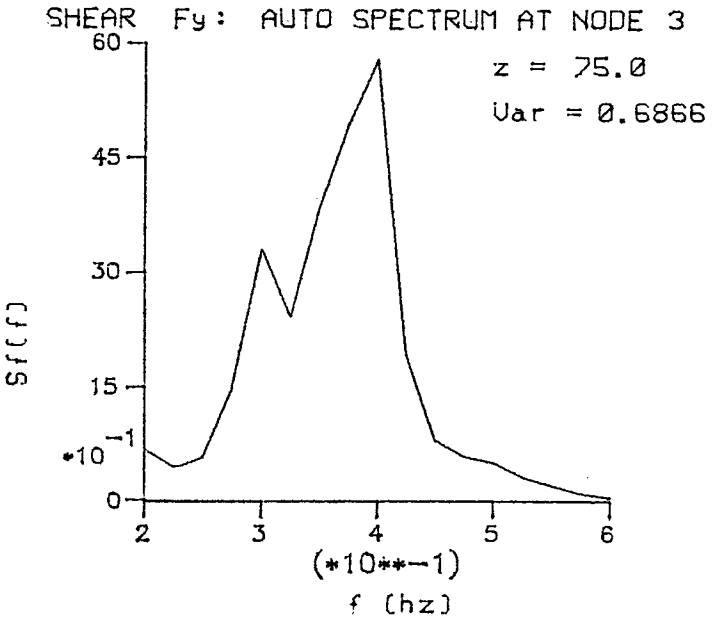

Figure 21. Vertical Structural Shear Force Auto Spectrum at Mid-Point in KIP^2 S

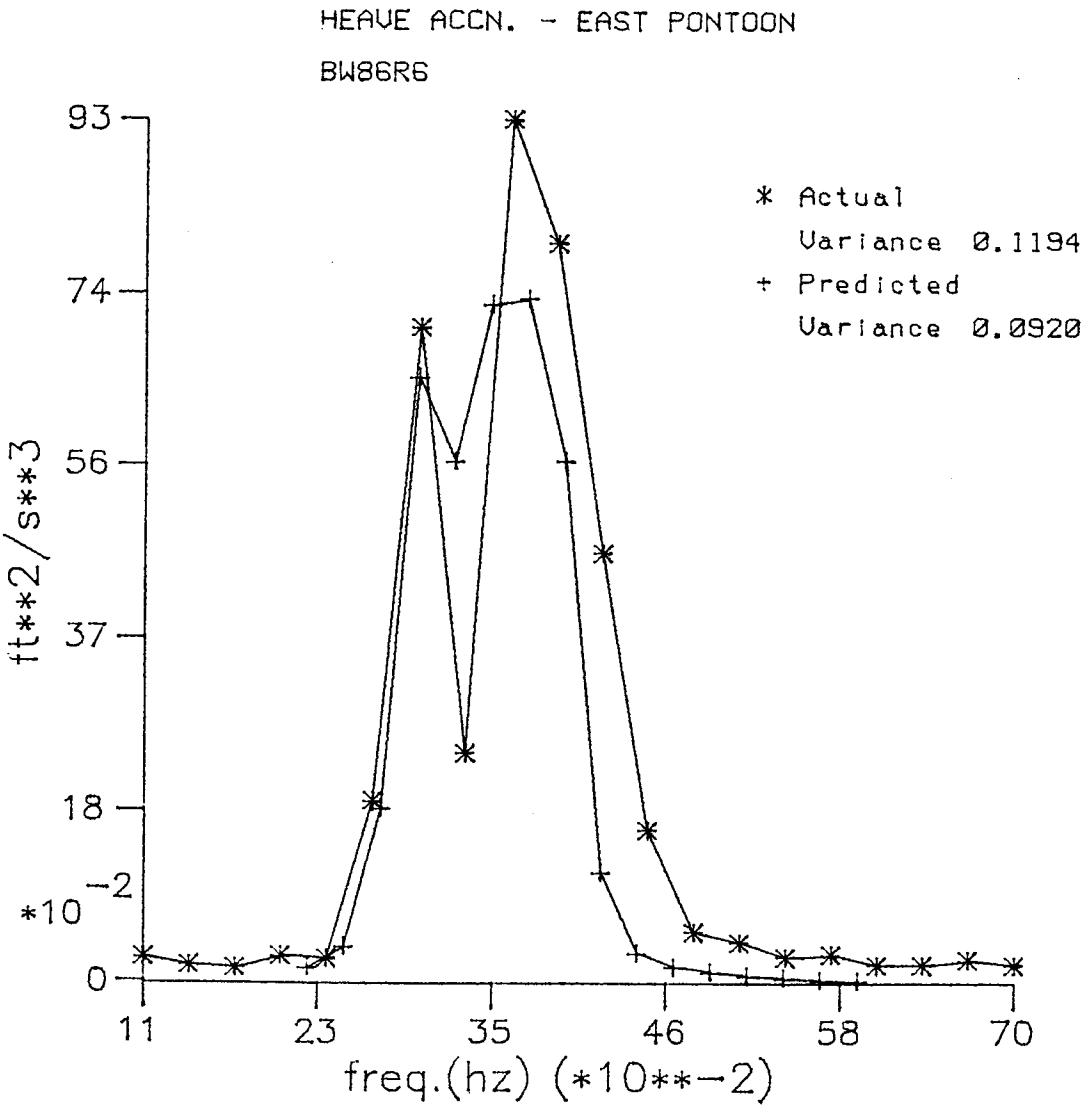

Figure 22. Predicted and Measured Heave Accelleration Auto Spectrum - East Pontoon